The Plant Cell, Vol. 21: 1473–1494, May 2009, www.plantcell.org © 2009 American Society of Plant Biologists

The Ethylene Receptor ETR2 Delays Floral Transition and Affects Starch Accumulation in Rice [W]

Hada Wuriyanghan,[1] Bo Zhang,[1] Wan-Hong Cao,[1,2] Biao Ma, Gang Lei, Yun-Feng Liu, Wei Wei, Hua-Jun Wu, Li-Juan Chen, Hao-Wei Chen, Yang-Rong Cao, Si-Jie He, Wan-Ke Zhang, Xiu-Jie Wang, Shou-Yi Chen, and Jin-Song Zhang[3]

Plant Gene Research Center, National Key Lab of Plant Genomics, Institute of Genetics and Developmental Biology, Chinese Academy of Sciences, Beijing 100101, China

Ethylene regulates multiple aspects of plant growth and development in dicotyledonous plants; however, its roles in monocotyledonous plants are poorly known. Here, we characterized a subfamily II ethylene receptor, ETHYLENE RESPONSE2 (ETR2), in rice (*Oryza sativa*). The ETR2 receptor with a diverged His kinase domain is a Ser/Thr kinase, but not a His kinase, and can phosphorylate its receiver domain. Mutation of the N box of the kinase domain abolished the kinase activity of ETR2. Overexpression of *ETR2* in transgenic rice plants reduced ethylene sensitivity and delayed floral transition. Conversely, RNA interference (RNAi) plants exhibited early flowering and the *ETR2* T-DNA insertion mutant *etr2* showed enhanced ethylene sensitivity and early flowering. The effective panicles and seed-setting rate were reduced in the *ETR2*-overexpressing plants, while thousand-seed weight was substantially enhanced in both the *ETR2*-RNAi plants and the *etr2* mutant compared with controls. Starch granules accumulated in the internodes of the *ETR2*-overexpressing plants, but not in the *etr2* mutant. The *GIGANTEA* and *TERMINAL FLOWER1/CENTRORADIALIS* homolog (*RCN1*) that cause delayed flowering were upregulated in *ETR2*-overexpressing plants but downregulated in the *etr2* mutant. Conversely, the α-amylase gene *RAmy3D* was suppressed in *ETR2*-overexpressing plants but enhanced in the *etr2* mutant. Thus, ETR2 may delay flowering and cause starch accumulation in stems by regulating downstream genes.

INTRODUCTION

The gaseous plant hormone ethylene plays important roles in multiple aspects of plant growth and development, including seed germination, hypocotyl elongation, root hair initiation, leaf and flower senescence, fruit ripening, and organ abscission (Abeles et al., 1992). It is also involved in plant responses to biotic and abiotic stresses, such as pathogen attack, wounding, hypoxia, and drought stress (Morgan and Drew, 1997). However, the role of ethylene in plants appears to be multifunctional in terms of growth stimulation and disease resistance (Pierik et al., 2006; van Loon et al., 2006). Through analysis of a series of ethylene response mutants of *Arabidopsis thaliana*, the backbone of the ethylene signaling pathway has been established and the major components have been identified (Bleecker and Kende, 2000; Wang et al., 2002; Guo and Ecker, 2004; Chen et al., 2005; De Paepe and Van Der Straeten, 2005). These components include the ethylene receptors, the protein kinase CONSTITUTIVE TRIPLE RESPONSE1 (CTR1), the membrane protein ETHYLENE-INSENSTIVE2 (EIN2), and the downstream transcription factors EIN3, EIN3-LIKE1 (EIL1), and ETHYLENE RESPONSE FACTOR1 (ERF1). EIN3 is quickly degraded in the absence of ethylene through an ubiquitin/proteasome pathway mediated by two F box proteins, EIN3 BINDING F-BOX1 (EBF1) and EBF2 (Guo and Ecker, 2003; Potuschak et al., 2003; Gagne et al., 2004). *EBF1* and *EBF2* mRNA levels can be regulated indirectly by exoribonuclease XRN4/EIN5 (Olmedo et al., 2006; Potuschak et al., 2006). EIN2 stability is also disrupted by two F box proteins, EIN2 TARGETING PROTEIN1 (ETP1) and ETP2 (Qiao et al., 2009). New components of the ethylene signaling pathway have been proposed, and these components may either fill the gaps in the established ethylene signaling pathway or represent new branches of this pathway (Alonso et al., 2003; Larsen and Cancel, 2003; Moshkov et al., 2003; Quaked et al., 2003; Hass et al., 2004; Yoo et al., 2008).

Ethylene receptors are the first component in ethylene signaling and can be classified into two subfamilies, subfamily I and subfamily II. In *Arabidopsis*, subfamily I has two members, whereas subfamily II has three members (Klee, 2004; Chen et al., 2005; Chen and Zhang, 2006; Wang et al., 2006; Hall et al., 2007). All of the *Arabidopsis* and tomato (*Solanum lycopersicum*) receptors can bind ethylene, and the important regions for ethylene binding of *Arabidopsis* ETR1 have been identified in the transmembrane domain (Schaller and Bleecker, 1995; Rodriguez et al., 1999; O'Malley et al., 2005). Ethylene binding activity is confined to land plants, *Chara*, and a group of cyanobacteria (Wang et al., 2006). Ethylene negatively regulates the functions of ethylene receptors (Hua and Meyerowitz, 1998). Ethylene receptors appear to be localized in membrane systems, such as the endoplasmic reticulum (Chen et al., 2002, 2007; Xie et al., 2003; Ma et al., 2006; Dong et al., 2008). ETR1, a subfamily I member, has histidine kinase

[1] These authors contributed equally to this work.
[2] Current address: Syngenta Biotechnology (China) Co., Ltd., Zhongguancun Life Science Park, Changping District, Beijing 102206, China.
[3] Address correspondence to jszhang@genetics.ac.cn.
The author responsible for distribution of materials integral to the findings presented in this article in accordance with the policy described in the Instructions for Authors (www.plantcell.org) is: Jin-Song Zhang (jszhang@genetics.ac.cn).
[W] Online version contains Web-only data.
www.plantcell.org/cgi/doi/10.1105/tpc.108.065391

activity, whereas tobacco (*Nicotiana tabacum*) subfamily II members NTHK1 (*Nicotiana tabacum* histidine kinase1) and NTHK2, and other *Arabidopsis* receptors, have Ser/Thr kinase activities (Xie et al., 2003; Moussatche and Klee, 2004; Zhang et al., 2004). The NTHK2 and ETHYLENE RESPONSE SENSOR1 (ERS1) receptors also have histidine kinase activities in the presence of Ca^{2+} and Mn^{2+}, respectively (Moussatche and Klee, 2004; Zhang et al., 2004). The ETR1 kinase domain has substantial roles in the regulation of ethylene responses and seedling growth recovery. However, whereas His kinase activity has little or no role in response to ethylene, it has a significant role in growth recovery (Wang et al., 2003; Binder et al., 2004; Qu and Schaller, 2004). Signal transmission by the ETR1 N terminus is dependent on the other subfamily I members (Xie et al., 2006), and the ETR1 receptor function can be regulated by a membrane protein, REVERSION-TO-ETHYLENE SENSITIVITY1, and a copper transporter, RESPONSIVE-TO-ANTAGONIST1 Hirayama et al., 1999; Resnick et al., 2006, 2008; Zhou et al., 2007; Dong et al., 2008). Recently, two studies have shown that ethylene receptor degradation represents a mechanism for regulating ethylene responses (Chen et al., 2007; Kevany et al., 2007). Formation of ethylene receptor dimers and/or higher-order receptor complexes also regulates ethylene signal output (Gao et al., 2008).

Ethylene receptor genes can be induced by various abiotic stresses (Zhang et al., 1999a, 2001a, 2001b). Overexpression of the tobacco ethylene receptor NTHK1 results in large rosettes or seedlings, reduced ethylene sensitivity, and increased salt sensitivity in transgenic plants (Xie et al., 2002; Cao et al., 2006; Zhou et al., 2006a). NTHK1 affects salt stress responses by alternating the expression pattern of the gene encoding the NAC transcription factor or of other relevant genes (He et al., 2004, 2005; Cao et al., 2006, 2007; Zhou et al., 2006a). Ethylene receptors also regulate plant defense responses (Knoester et al., 1998; Ciardi et al., 2000; O'Donnell et al., 2003). In addition to stress responses, ethylene receptors are highly expressed in reproductive organs and may be involved in reproductive development (Hua et al., 1998; Sato-Nara et al., 1999; Tieman et al., 2000; Yamasaki et al., 2000; Zhang et al., 2001a, 2001b; Klee, 2002, 2004; Xie et al., 2002; Rieu et al., 2003; Zhou et al., 2006a).

In monocots, ethylene receptor genes have been identified in wheat (*Triticum aestivum*) and maize (*Zea mays*) (Ma and Wang, 2003; Gallie and Young, 2004). In rice (*Oryza sativa*), ethylene receptor genes, *EIN2*-like and *EIN3*-like, have also been cloned, and the functions of the *EIN2*-like and *EIL1* genes have been analyzed (Cao et al., 2003; Cao, 2004; Jun et al., 2004; Watanabe et al., 2004; Yau et al., 2004; Mao et al., 2006). The rice ethylene receptor gene family has five members, including *Protein Kinase1* (*PK1*)/*ETR2*/*ETHYLENE RESPONSE2 like1* (*ERL1*), *PK2*/*ETR3*, *PK3*/*ETR4*, *ERS1*, and *ERS2*. ERS1 and ERS2 belong to subfamily I, whereas the other three belong to subfamily II. Expression of these genes can be affected by various stresses and hormone treatments (Cao et al., 2003; Cao, 2004; Watanabe et al., 2004; Yau et al., 2004). Alternative spliced forms of these receptors have also been reported after analysis of the whole rice genome (Pareek et al., 2006). Although rice ethylene receptor genes have been identified, the biochemical properties of the proteins are not known. The function of the receptors in plant growth and development remains unclear.

In this study, we further characterized the *PK1*/*ETR2*/*ERL1* gene from rice (Cao, 2004; Watanabe et al., 2004; Yau et al., 2004). For simplicity, the name ETR2 was chosen to represent the three names of this ethylene receptor. The kinase activity of the ETR2 protein was investigated. The roles of this receptor protein in rice plant growth and reproductive transition were analyzed using overexpression and RNA interference (RNAi) approaches. The *ETR2* T-DNA insertion mutant, *etr2*, was further identified and studied. Our results indicate that ETR2 has Ser/Thr kinase activity and can phosphorylate its receiver domain. In rice, ETR2 reduces ethylene sensitivity, delays the transition from the vegetative stage to the floral stage, and affects starch accumulation.

RESULTS

Structural Features of the ETR2 Ethylene Receptor in Rice

Based on the SMART analysis and comparison with ethylene receptors from *Arabidopsis*, tobacco, and maize, the putative domains in rice ETR2 were predicted. ETR2 contains four hydrophobic regions, a GAF domain (amino acid positions 190 to 349), a putative kinase domain (amino acid positions 375 to 615), and a receiver domain (amino acid positions 640 to 756) (Figure 1A). The first hydrophobic region (amino acid positions 1 to 26) probably represents a signal peptide, whereas the other three hydrophobic regions (amino acid positions 58 to 78, 86 to 108, and 115 to 137) represent transmembrane domains. The putative kinase domain consists of two subdomains, an H-containing domain (HIS, amino acid positions 375 to 440) and an ATP binding domain (ATP, amino acid positions 487 to 615) (Figures 1A and 1B). HIS is a dimerization and phosphoacceptor subdomain in bacterial histidine kinases, whereas an ATP binding subdomain is found in several ATP binding proteins, such as histidine kinase, DNA gyrase B, topoisomerases, and heat shock protein HSP90 (Parkinson and Kofoid, 1992; Robinson et al., 2000). The receiver domain (RD; amino acid positions 640 to 756) contains a putative phosphoacceptor site (D692) that is normally phosphorylated by a histidine kinase in bacteria (Parkinson and Kofoid, 1992).

The rice ETR2 kinase domain was compared with those from other ethylene receptors or homologs (Figure 1B). In the H motif of the HIS domain, rice ETR2 had a D385, which was different from the phosphorylation site H353 in ETR1 of *Arabidopsis* (Gamble et al., 1998) or residues in other proteins in the corresponding region. However, maize ETR2 had a D400 residue at the corresponding position. Seven residues downstream of the D385 in rice ETR2, an H392 residue was identified, which was highly conserved at the corresponding position among all the proteins compared (Figure 1B). However, this residue was not required for the kinase activity observed in NTHK2, *Arabidopsis* ETR2, or EIN4 (Moussatche and Klee, 2004; Zhang et al., 2004). In the ATP subdomain of *Arabidopsis* ETR1 and other histidine kinases, four motifs, including the N, G1, F, and G2 boxes, have been identified (Robinson et al., 2000; Parkinson and Kofoid, 1992; Chang et al., 1993). However, in rice ETR2 and in the other subfamily II members compared, the G1, F, and G2 boxes were more divergent than those in *Arabidopsis* ETR1, whereas the N box and the nearby residues were relatively conserved (Figure 1B). The residues

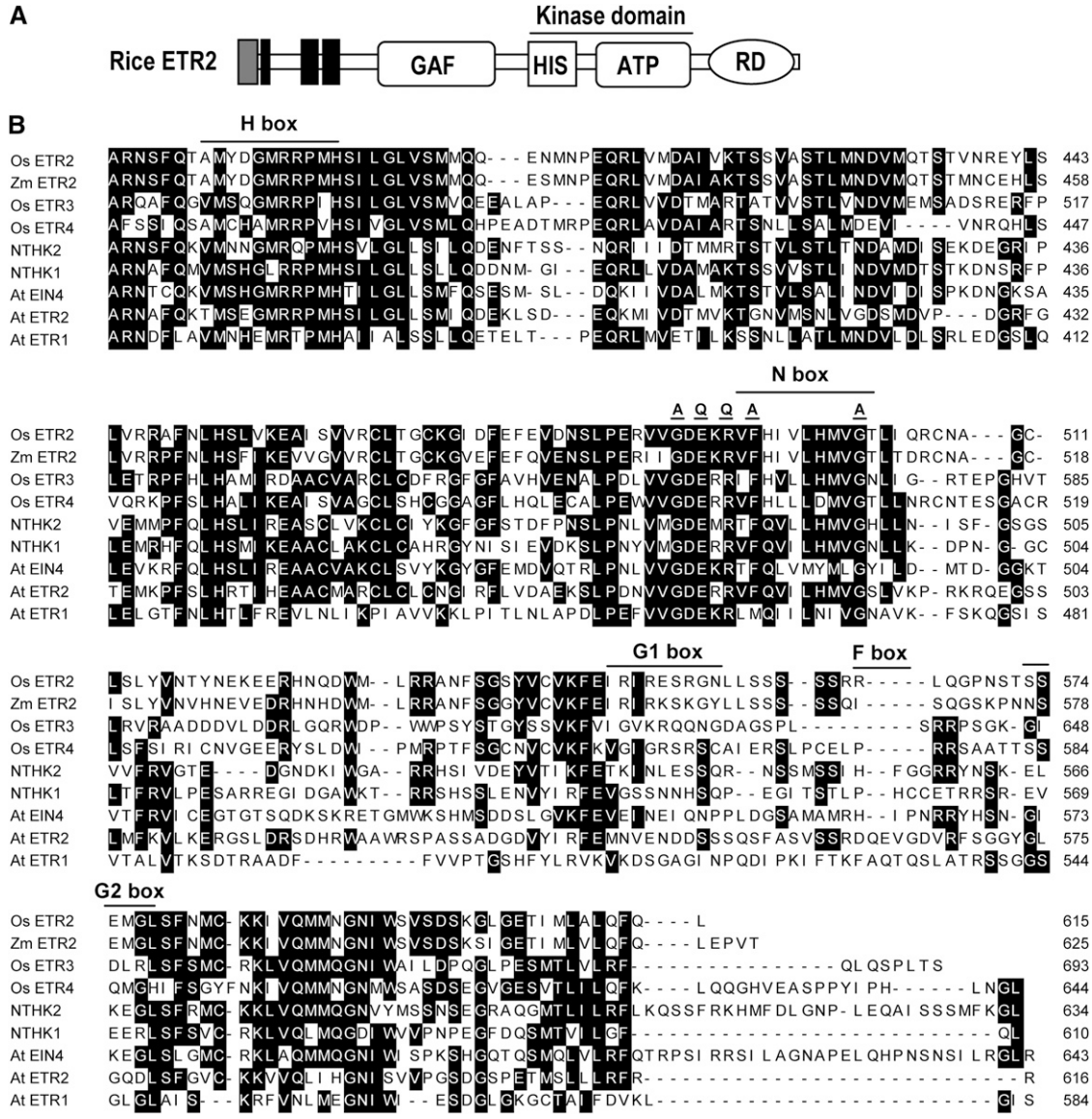

Figure 1. Structural Features of Rice ETR2 and Alignment of the Amino Acid Sequence of the Kinase Domain with That of Other Ethylene Receptors.

(A) Schematic representation of the rice ETR2 structure. The first box (gray) indicates a putative signal peptide. The next three boxes (black) indicate putative transmembrane domains. The GAF domain, the kinase domain, including the HIS and ATP subdomains, and the RD domain are also indicated.
(B) Alignment of the amino acid sequences of the ethylene receptor kinase domains of various ethylene recpetors. The positions of the H, N, G1, F, and G2 box are indicated on top of the sequence based on the corresponding boxes from *Arabidopsis* ETR1. The amino acids shaded in black are identical to each other. Five mutated amino acids (G to A, E to Q, R to Q, F to A, and G to A) upstream of and within the N box are also indicated, and the mutated protein N was used for kinase analysis in Figure 2. At ETR1, At ETR2, and At EIN4 are from *Arabidopsis*. NTHK1 and NTHK2 are from tobacco. Zm ETR2 is from maize. The Os ETR2/Os PK1, Os ETR3/Os PK2, and Os ETR4/Os PK3 receptors are from rice.

G487, D488, E489, R491, F493, M499, and G501 in rice ETR2 may play roles in the regulation of receptor activity.

Kinase Activity of the ETR2 Protein

Ethylene receptors in dicotyledonous plants have been found to possess kinase activities; *Arabidopsis* ETR1 has His kinase activity, whereas the other receptors tested mainly have Ser/Thr kinase activities. *Arabidopsis* ERS1 and tobacco NTHK2 also have His kinase activities in the presence of Mn^{2+} and Ca^{2+}, respectively (Gamble et al., 1998; Xie et al., 2003; Moussatche and Klee, 2004; Zhang et al., 2004). Here, we investigated the kinase activity of ETR2 from monocotyledonous rice plants to establish if they have different biochemical properties from those found in dicotyledonous plants. Four truncated versions of ETR2 were expressed as glutathione *S*-transferase (GST) fusions in

bacterial cells (Figures 2A and 2B). The wild-type fusion contained the GAF domain, the HIS domain, and the ATP domain. The N protein had five mutations (G487A, E489Q, R491Q, F493A, and G501A) in the N box of the wild-type protein. The ΔATP fusion contained the GAF domain and the HIS domain. The RD fusion only contained the receiver domain. These purified proteins displayed apparent molecular masses consistent with their corresponding predicted molecular masses when analyzed by SDS-PAGE (Figure 2B). It should be noted that in the wild-type, N, and ΔATP proteins, a similar protein band of ~50 kD was

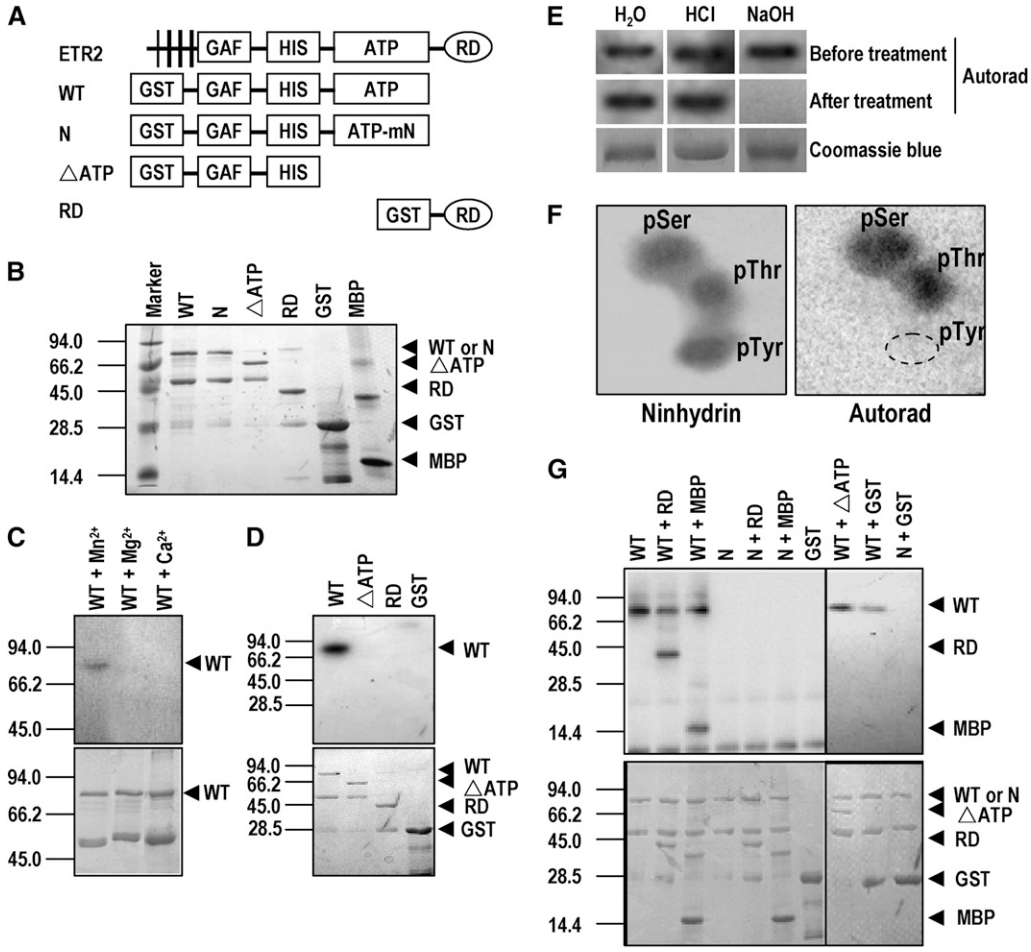

Figure 2. Phosphorylation Assay of the ETR2 Protein.

(A) Various truncated versions of the ETR2 protein expressed in bacteria. The full-length ETR2 protein was placed on the top for comparison. The N harbors mutations of five amino acids near the N box in the subdomain ATP-mN. GST was used as an affinity tag.

(B) Purification of the truncated versions of the ETR2 GST-fusion protein. A common protein band (~50 kD) was noted in the wild-type, N, and ΔATP protein preparations, and this band represented a degradation product of their original proteins, as established by Matrix Assisted Laser Desorption/Ionization Time-of-Flight (MALDI-TOF) Mass Spectrometry analysis. The GST protein and the commercial MBP protein were also included for comparisons. Proteins were separated by SDS-PAGE and stained with Coomassie blue.

(C) Autophosphorylation of the ETR2 kinase domain. The GST-fusion wild type was incubated with [γ-^{32}P]ATP in the presence of 5 mM Mn^{2+}, 5 mM Mg^{2+}, or 5 mM Ca^{2+}. Phosphorylated proteins were separated by SDS-PAGE, transferred onto a PVDF membrane, and autoradiographed (top) or stained with Coomassie blue (bottom).

(D) Autophosphorylation assay of various domains of ETR2. Assays were performed in the presence of 5 mM Mn^{2+}. Other procedures are the same as those in **(C)**.

(E) Hydrolytic stability of the phosphorylated ETR2. The wild type was autophosphorylated in the presence of Mn^{2+} and then the phosphorylated wild type was subjected to treatments with water, HCl, or NaOH.

(F) Phosphoamino acid analysis of the phosphorylated ETR2. The positions of the phosphoamino acids were identified by spraying with ninhydrin (left), and the labeled residues (pSer, pThr, and pTyr) were revealed by autoradiography (right).

(G) Mutation and substrate analysis of the ETR2 kinase domain. The wild-type or N mutant was incubated under phosphorylating conditions with RD or MBP. After separation by SDS-PAGE, the phosphorylated proteins were subjected to autoradiography (top) or Coomassie blue staining (bottom). Numbers on the left indicate the sizes of the protein markers (kD) for **(C)**, **(D)**, and **(G)**.

usually observed (Figure 2B). This band represented a degradation product of their original proteins.

The wild-type protein was subjected to a phosphorylation assay through incubation with [γ-^{32}P]ATP. In the presence of Mn^{2+}, ^{32}P was incorporated into the wild-type fusion protein (Figure 2C). However, in the presence of Mg^{2+} and Ca^{2+}, ^{32}P incorporation was not found. This result indicates that the wild-type autophosphorylation requires Mn^{2+} as a cofactor. Other truncated ETR2 proteins were also compared for their phosphorylation ability in the presence of Mn^{2+}. Only the wild type had the ability to autophosphorylate, whereas the ΔATP, RD, and GST did not have such an ability (Figure 2D). This result indicates that the ATP domain is required for the wild-type phosphorylation. To examine which classes of residues are phosphorylated, the phosphorylated wild-type protein was transferred onto polyvinylidene difluoride (PVDF) membrane and treated with acid or base to test its hydrolytic stability. The wild-type protein was stable under acidic treatment but sensitive to base treatment, and overnight treatment with NaOH abolished the phosphorylation level completely (Figure 2E). These results imply that the phosphorylated wild type contained phosphoserine, phosphothreonine, or phosphotyrosine, but not phosphohistidine. The phosphorylated wild-type protein was also subjected to phosphoamino acid analysis by two-dimensional thin-layer chromatograph electrophoresis, which revealed that the phosphorylated ETR2 protein contained phosphoserine and phosphotheronine (Figure 2F). The N box of the wild type was further mutated, and the mutant version N did not have any ^{32}P incorporation, suggesting that the N box is important for the phosphorylation and that kinase activity is intrinsic to the wild type (Figure 2G).

The receiver domain of two-component proteins in bacteria and yeast usually accepts the phosphate group from histidine kinase (Parkinson and Kofoid, 1992; Wurgler-Murphy and Saito, 1997; Robinson et al., 2000). Thus, we investigated if the wild type can phosphorylate RD and the universal substrate myelin basic protein (MBP) in vitro. MBP has been used as a substrate to examine kinase activities of protein kinases and ethylene receptors (Cicirelli et al., 1988; Xie et al., 2003; Zhang et al., 2004). Our results indicate that the wild-type protein can phosphorylate both RD and MBP (Figure 2G). However, the mutant protein N did not phosphorylate the two proteins, suggesting that the N box is required for substrate phosphorylation. The wild type was also incubated with ΔATP in the presence of [γ-^{32}P]ATP to test if the wild type could phosphorylate other domains. The wild type could not phosphorylate ΔATP, suggesting that the phosphorylated residues in the wild type are likely in the ATP subdomain and not in the GAF or HIS subdomains (Figure 2G). Neither the wild type nor N could phosphorylate GST, and GST itself did not have any ^{32}P incorporation (Figure 2G).

Overexpression of ETR2 Reduces Ethylene Sensitivity in Transgenic Rice

To study the roles of ETR2 in rice growth and development, we made two constructs, pBIN438-OsETR2 and pZH01-OsETR2-RNAi, and transferred them into rice (TP309) via *Agrobacterium tumefaciens*–mediated transformation. The pBIN438-OsETR2 construct harbored the full-length genomic gene of *ETR2* under the control of the double 35S promoter with an enhancer. The pZH01-OsETR2-RNAi construct contained two inverted repeats of the partial *ETR2* gene and was used for inhibiting *ETR2* gene expression (Figure 3A). Forty-one T0 overexpression lines and 20 T0 RNAi lines were obtained. From these, T2 or T3 homozygous lines (8-2, 12-1, 17-1, and 56-4, with one to two insertions) with higher expression of the *ETR2* gene and two homozygous independent RNAi lines (41-4 and 66-1, with one and two insertions, respectively) were used for further analysis (Figure 3B). The two RNAi lines had reduced, but not eliminated, expression of *ETR2*. Generally, *ETR2* was expressed in rice plants at a very low level (Figure 3B).

Since ETR2 is a homolog of ethylene receptors, we hypothesized that overexpression or reduction in *ETR2* levels would alter ethylene sensitivity in the transgenic plants. We analyzed the response of the transgenic seedlings upon 1-aminocyclopropane-1-caroxylic acid (ACC; ethylene biosynthesis precursor) treatment. Root growth of etiolated wild-type rice seedlings (wild type) was inhibited in response to increasing concentrations of ACC, whereas shoot growth was not significantly affected (Figure 3C). In the four lines overexpressing *ETR2*, root lengths were only slightly reduced upon ACC treatment compared with the corresponding wild-type controls (Figure 3C, top and bottom left panels). In the two RNAi lines with reduced *ETR2* expression, root lengths were similar to that of the wild-type plants in response to ACC treatment (Figure 3C, top and bottom right panels). Shoot lengths of the overexpression lines and the RNAi lines were not significantly different from those of the wild-type controls (Figure 3C, top panels). These results indicate that rice roots are more sensitive to ACC treatment than are rice shoots and that overexpression of *ETR2* conferred reduced ethylene sensitivity in transgenic rice plants. Partial reduction of the *ETR2* level had limited effects on ethylene sensitivity.

Ethylene can promote the growth of rice coleoptiles (Ku et al., 1970). We examined the sensitivity of the transgenic rice plants to ethylene by testing for the promotion of coleoptile growth. At higher ethylene concentrations (50 ppm), the transgenic plants overexpressing *ETR2* exhibited significantly shorter coleoptiles than wild-type plants (Figure 3D), indicating that overexpression of *ETR2* conferred reduced ethylene sensitivity in the regulation of coleoptile growth. The RNAi plants showed no significant changes in coleoptile length in comparison with the wild-type plants.

Phenotypes of Transgenic Rice Plants with Altered *ETR2* Expression

We investigated the phenotypic changes in transgenic plants exhibiting increased or decreased *ETR2* expression. Four lines overexpressing *ETR2* had shorter seedlings than control plants after 5 d of germination (Figure 4A) or 50 d of growth in the field (Figure 4B). However, seedlings from the two RNAi lines exhibited no significant difference in seedling length compared with control seedlings under both conditions. These results suggest that ETR2 has an inhibitory effect on rice seedling elongation.

Observations of growth of the transgenic rice plants in field conditions revealed that *ETR2*-overexpressing lines had delayed flowering. We thus examined panicle development in these

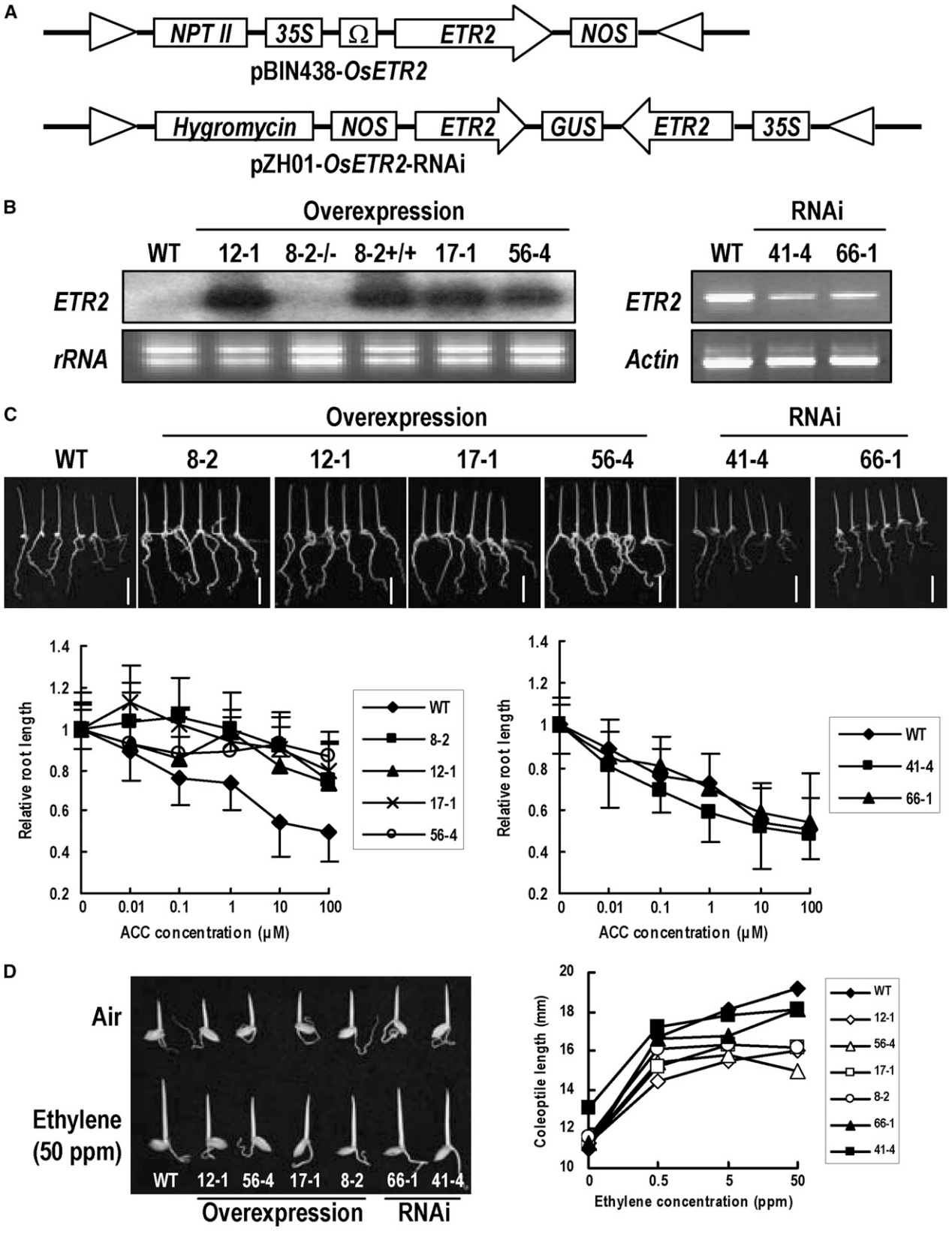

Figure 3. Ethylene Sensitivity of *ETR2* Transgenic Rice Plants.

transgenic plants more closely. At the stage of panicle development, the two *ETR2*-RNAi plants had more well-developed panicles than the wild-type plants. However, the four lines overexpressing *ETR2* had only one to two young panicles developed (Figure 4C). Heading dates of field-grown plants were also recorded and three *ETR2*-overexpressing lines (8-2, 17-1, and 56-4) had a heading date about 1 week later than control plants, whereas line 12-1 showed a heading time nearly 2 weeks later than controls. Two RNAi lines, 41-4 and 66-1, exhibited a heading time 3 to 4 d earlier than controls (Figure 4D). These results indicate that ETR2 may delay plant transition from the vegetative stage to the reproductive stage.

The phenotype of field-grown plants at the mature stage was further observed. Control plants and the two RNAi lines all had downward panicles, whereas *ETR2*-overexpressing lines had erect panicles (Figure 4E). In overexpressing line 12-1, panicles were barely emerged, and leaves were still very green. These results suggest that ETR2 delays the development of plants to maturity. The length of each internode was also measured when plants stopped elongating after maturation. Two RNAi lines were not different from controls in the length of all four internodes (Figure 4F). However, four *ETR2*-overexpressing lines had shorter internodes compared with control plants (Figure 4F). The overall height of three *ETR2*-overexpressing lines (12-1, 17-1, and 56-4) was shorter than controls. The two RNAi lines were of similar heights as the control line (Figure 4G). These results suggest that ETR2 suppresses internode elongation and delays panicle development in rice.

Yield-Related Traits of the Transgenic Rice Plants with Altered *ETR2* Expression

At maturity, the control and the two RNAi lines had yellow and drooping panicles, whereas four *ETR2*-expressing lines had yellow-green or green but upright panicles (Figure 5A). After harvest, the ratio of effective tillers (tillers bearing panicles) was decreased in the *ETR2*-overexpressing line 12-1 (Figure 5B). However, this ratio was only slightly reduced or not significantly changed in other *ETR2*-overexpressing lines or in the two RNAi lines. The effective panicles (panicle having at least one full-sized grain) and the seed-setting rates were also evaluated. Both parameters were reduced in all four *ETR2*-overexpressing lines, whereas the two RNAi lines had no significant difference compared with the controls (Figure 5B). These results indicate that ETR2 significantly affects panicle development and seed set.

Since ETR2 delays floral transition of rice plants, this may cause the low seed-setting rate of *ETR2*-overexpressing lines. Alternatively, ETR2 may extend the maturation process and grain-filling process, leading to low seed-set in the normal harvest season. To distinguish between these two possibilities, control plants (WT2) were further grown 18 d later than normal control plants (WT1) and transgenic plants. We found that the late-grown WT2 had the same heading date as the *ETR2*-overexpressing line 12-1, which had a severe phenotype. However, the seed-setting rate of this late-grown WT2 remained similar to that of the normal WT1 (Figure 5C). These results indicate that late flowering of the late-grown WT2 did not significantly change its seed-setting rate, suggesting that the low seed-set in *ETR2*-overexpressing lines was not due to late heading, but likely due to the ETR2 roles in extension of the seed ripening process.

Seed phenotypes were compared, and seed coats from the two RNAi lines were yellow, whereas seed coats from control plants and the four *ETR2*-overexpressing lines had brown regions, suggesting that seeds from the two RNAi lines were riper than seeds from other lines (Figure 5D). The thousand-seed weights were substantially higher in the two RNAi lines 41-4 and 66-1 grown both in Beijing and Hainan compared with controls (Figure 5E). However, four *ETR2*-overexpressing lines had lower thousand-seed weight or no change in this parameter.

Starch Accumulation in the Internode of the *ETR2*-Overexpressing Rice Plants

Cross sections of the internodes of transgenic plants showed that starch granule accumulation was altered relative to the

Figure 3. (continued).

(A) Constructs used for rice transformation. Overexpression of the *ETR2* gene (top) and RNAi inhibition of *ETR2* (bottom).

(B) *ETR2* gene expression in overexpressing plants and RNAi plants. In the left panel, overexpression was revealed by RNA gel blot analysis. In the right panel, RT-PCR analysis was performed and the *actin* gene was amplified as a control; one of three consistent biological replicates is shown. The 8-2$^{-/-}$ and the 8-2$^{+/+}$ represent T2 segregated wild-type and homozygous *ETR2* transgenic plants, respectively, from seeds of the heterozygous T1 plants. All other lines are T2 homozygous lines. WT indicates control TP309.

(C) Response of etiolated transgenic rice seedlings to ACC treatment. In each of the top row of panels, 3-d-old seedlings were treated with ACC at concentrations of 0, 0.01, 0.1, 1, 10, and 100 μM (from left to right), respectively for 7 d. T3 seeds were used for the assay. The bottom part indicates relative root growth upon ACC treatment. The root length of the corresponding seedlings at zero point (3-d-old seedlings were further grown in water for 7 d) was set to 1, and all the other values were compared with it. Each data point represents the average of 15 to ~20 seedlings, and bars indicate SD. Only one SD was shown for simplicity. The left panel is for overexpressing lines, and the difference between the four overexpressing lines and the wild type is significant ($P < 0.05$) at 1, 10, and 100 μM. At 0.1 μM, the 8-2 and 17-1 points are also significantly different from the wild type ($P < 0.05$). The right panel is for RNAi lines. Bars = 4 cm.

(D) Coleoptile growth of the transgenic rice seedlings under ethylene treatment. The photograph on the left was taken 3 d after seed germination in the dark at 25°C with 50 ppm ethylene treatment. The right panel indicates coleoptile growth in response to ethylene. Each data point represents the average of 15 to ~20 seedlings. Among all the data points, the largest standard error was 0.55, and these are not shown for simplicity. The difference in coleoptile length between the wild type and the four overexpressing lines is significant ($P < 0.05$) at 50 ppm.

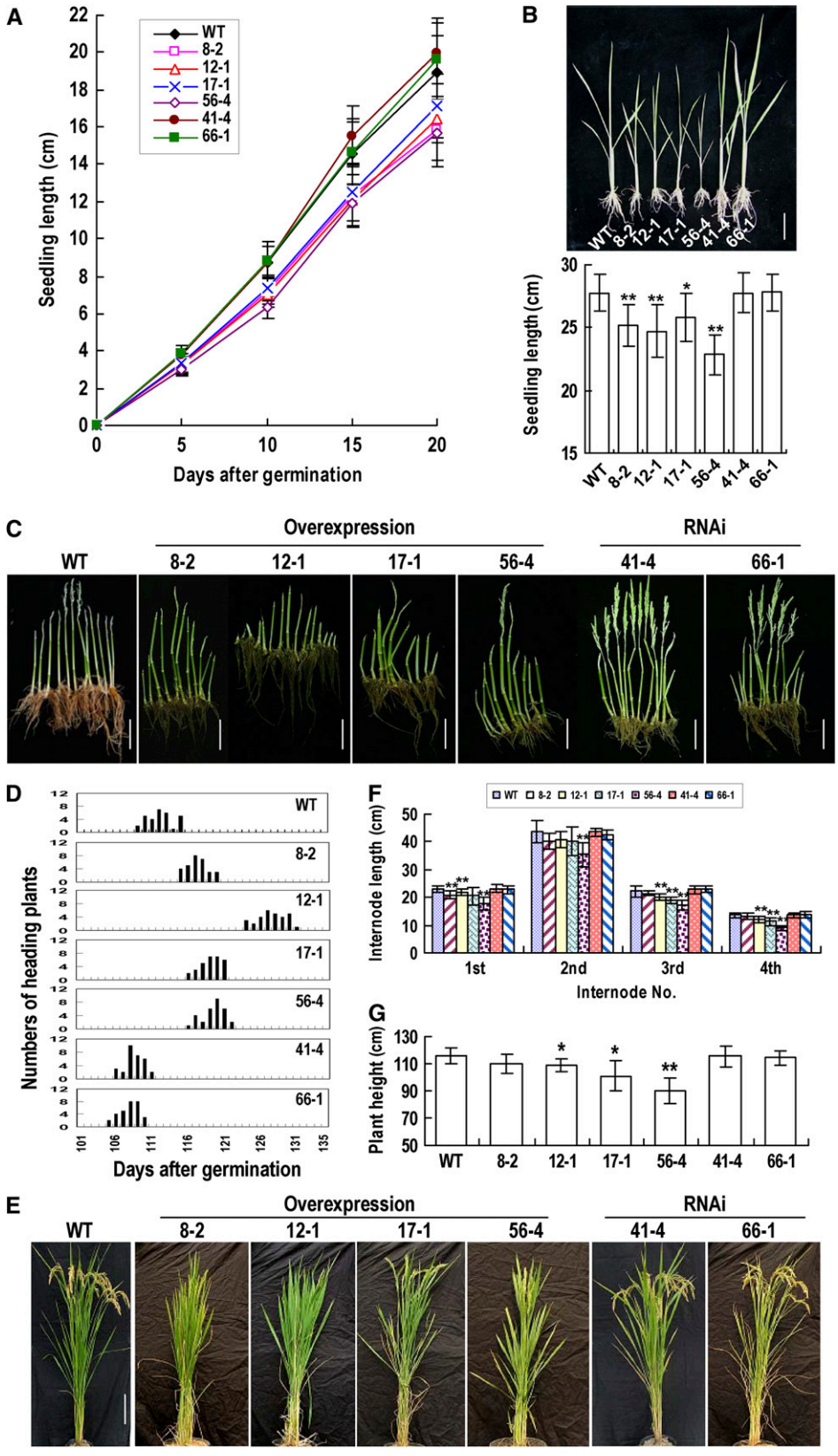

Figure 4. Phenotype of the *ETR2*-Overexpressing Plants and the RNAi Lines.

wild type. At the same growing period of 162 d, the *ETR2*-overexpressing line 12-1 had more starch granules in all four internodes compared with the controls (Figure 6A). Consistently, the first internode of RNAi line 41-4 had fewer starch granules compared with the controls. However, other internodes of these RNAi plants showed no difference in numbers of starch granules. This result suggests that ETR2 promotes the accumulation of starch granules in internodes.

It is possible that the difference in starch accumulation between *ETR2*-overexpressing lines and the control plant was due to the difference in developmental stage. Thus, we measured numbers of starch granules in these plants that were at the same developmental stage of full heading, but with different growth time. The first internode of all four *ETR2*-overexpressing lines had higher average numbers of starch granules than control plants and the two RNAi lines (Figures 6B and 6C). However, in the other three internodes, no significant difference in number of starch granules was observed among the lines compared. Iodine staining further revealed that four *ETR2*-overexpressing lines had a high density of starch granules, whereas control plants and the two RNAi lines had a lower density of starch granules (Figure 6D). These results suggest that ETR2 may facilitate starch accumulation in the internodes of rice plants.

The ETR2 Receptor Regulates Gene Expression

To investigate if ETR2 affected rice growth and development by regulating downstream genes, we performed a microarray analysis using Affimetrix rice gene chips. Shoot apical meristems (SAMs) from field-grown rice plants, including control plants, the *ETR2*-overexpressing line 12-1, and the RNAi line 41-4, were used to isolate RNA for chip analysis. Compared with control plants, 57 genes were upregulated and 263 genes were downregulated in the *ETR2*-overexpressing line 12-1 (see Supplemental Data Sets 1 and 2 online). In the RNAi line 41-4, 157 genes were upregulated and 68 genes were downregulated compared with control plants (see Supplemental Data Sets 3 and 4 online). Through further comparison of genes that showed altered expression, we identified genes consistently regulated in the *ETR2*-overexpressing line 12-1 and the RNAi line 41-4 (see Supplemental Data Set 5 online). Among these, 63 genes were downregulated in the *ETR2*-overexpressing line but upregulated in the *ETR2*-RNAi line. By contrast, eight genes were upregulated in the overexpressing line but downregulated in the RNAi line. These analyses suggest that ETR2 mainly plays inhibitory roles on gene expression, and only 13% of the total regulated genes showed a reciprocal expression pattern in the overexpressing line and RNAi line. The microarray data were further analyzed using the GOEAST program (Zheng and Wang, 2008; http://omicslab.genetics.ac.cn/GOEAST/index.php). Flower development, and many other biological processes, cellular components, and molecular functions were found to be substantially affected in the *ETR2*-overexpressing line 12-1 and *ETR2*-RNAi line 41-4 (see Supplemental Figures 1 to 6 online).

Because ETR2 caused a late flowering phenotype in the overexpressing lines and its suppression in the RNAi lines resulted in early flowering, we chose several flowering-related genes (see Supplemental Data Set 6 online) from the microarray analysis, including *OsGI*, *RCN1*, MADS box genes, and *ONAC300*, and examined their expression in transgenic plants. *OsGI* and *RCN1* genes have been reported to cause late flowering or late transition to the reproductive stage in rice plants (Nakagawa et al., 2002; Hayama et al., 2003). MADS box genes and *NAC* genes have been found to promote the differentiation of flower organs (Aida et al., 1997, 1999; Rijpkema et al., 2007). *OsGI* was enhanced in the shoot apical meristem (SAM) of the two *ETR2*-overexpressing lines 8-2 and 12-1, but slightly decreased in the SAM of the two RNAi lines 41-4 and 66-1 compared with controls (Figure 7A). *OsGI* gene expression was further reduced in the panicles of control plants. *RCN1* gene expression was enhanced in the two *ETR2*-overexpressing lines. However, its expression was not significantly changed in the two RNAi lines compared with controls. Expression of two *MADS* genes and *ONAC300* was reduced in the two overexpressing lines, but not significantly altered in the two RNAi lines in comparison with control plants (Figure 7B). The *ETR2* gene was highly expressed in the SAM of the two *ETR2*-overexpressing lines, and 12-1 had higher expression than the 8-2 line (Figure

Figure 4. (continued).

(A) Seedling length of the *ETR2*-overexpressing lines (8-2, 12-1, 17-1, and 56-4) and the RNAi lines (41-4 and 66-1). T3 seeds were germinated and grown on wet cheesecloth for different periods of time, and the shoot length was measured. Each data point represents an average of 15 to 20 seedlings, and bars indicate SD.

(B) Shoot length of the transgenic seedlings grown in soil seed bed for 50 d. Top panel: phenotype of the transgenic seedlings. Bar = 5 cm. Bottom panel: comparison of the seedling lengths. The data are averages of 15 to 20 seedlings, and bars indicate SD.

(C) Comparison of the panicle development in various transgenic lines. The 100-d-old plants grown in the field were peeled, and the young panicles or the SAM tissue was photographed and compared. Bars = 10 cm.

(D) Heading time distributions of the transgenic rice plants grown in the field. During the heading period, the number of heading plants for each line was recorded each day and compared.

(E) Phenotypic comparison of the transgenic plants during the heading period. The rice plants had been grown in the field for 139 d. The plants from the transgenic lines and the wild type were carefully pulled out from the field and regrown in pots for photographing. Bar = 20 cm.

(F) Internode length of the transgenic rice plants in comparison with the control plants. From top to bottom, four internodes were measured before harvest. Each data point represents the average of 15 to 20 plants, and bars indicate SD.

(G) Comparison of plant height. Measurements were performed before harvest, and the data are an average of 30 plants. Bars indicate SD. For all the data, one asterisk indicates significant difference ($P < 0.05$), and two asterisks indicate extremely significant difference ($P < 0.01$) in comparison with the control value.

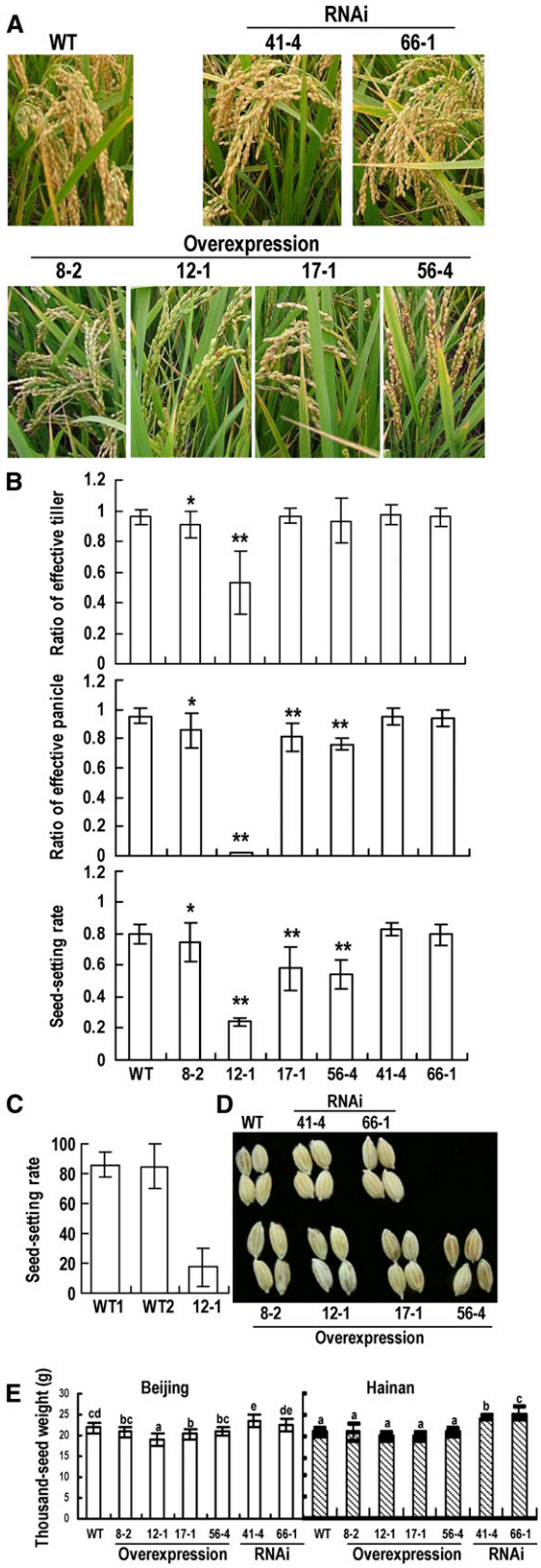

Figure 5. Yield-Related Traits of the *ETR2*-Overexpressing Rice Plants and the RNAi Plants in Comparison with the Control.

7A). All of these results indicate that ETR2 may promote *OsGI* and *RCN1* gene expression but inhibit *MADS5*, *MADS7*, and *ONAC300* expression, leading to the late heading phenotype in *ETR2*-overexpressing rice plants.

Since starch accumulation was altered in the *ETR2*-overexpressing lines, we studied expression of the α-amylase gene *RAmy3D*. α-Amylase catalyzes the hydrolysis of α-1,4 glucan bonds of amylase and amylopectin (Beck and Ziegler, 1989). *RAmy3D* expression was inhibited in the SAM of the two overexpressing lines but not significantly affected in the two RNAi lines compared with control plants (Figure 7C). This result suggests that ETR2 may inhibit starch degradation, leading to starch accumulation in internodes of the *ETR2*-overexpressing lines. A gene encoding a putative monosaccharide transporter was also identified from microarray analysis, and this gene was reduced in SAM of the overexpressing lines but enhanced in the two RNAi lines (Figure 7C). This expression pattern indicates that ETR2 may also inhibit genes responsible for sugar translocation.

Expression patterns of the above genes were further investigated in different organs of rice plants. The two *MADS* box genes, *RAmy3D*, and the putative monosaccharide transporter gene were mainly expressed in SAM and panicles, whereas *OsGI*, *RCN1*, and *ONAC300* were expressed in all organs examined (Figures 7A to 7C). These results suggest that the first four genes may function in SAM or the transition from the vegetative stage to the reproductive stage, whereas the last three genes may play roles in growth and development of multiple organs.

Previous studies have demonstrated functional compensation within the ethylene receptor family in tomato (Tieman et al., 2000). Thus, we examined whether alteration of *ETR2* gene expression would affect expression of the other ethylene receptor genes. Figure 7D showed that although the *ETR2* levels were elevated in the overexpressing lines and suppressed in the RNAi lines, no significant changes in expression of the other four

(A) Panicle morphology of transgenic plants. The plants were grown in the field for 157 d.

(B) Comparison of yield-related traits in transgenic plants and control plants. In the top panel, the effective tillers (ratio of the tillers having panicles to all the tillers) was compared. In the middle panel, the effective panicles (ratio of the panicles having at least one full-sized grain at maturity to all the panicles) was compared. Seed-setting rate in the different lines was compared in the bottom panel.

(C) Seed-setting rate of the severe *ETR2*-overexpressing line 12-1 in comparison with the control plants. WT1 indicates a normal control, whereas the WT2 indicates an 18-d-old late-grown control. The WT1 was sown at the same time as the 12-1 line, whereas the WT2 had the same heading date as the 12-1 line.

(D) Seed phenotype at harvest from various transgenic lines.

(E) Comparison of the thousand-seed weight from various transgenic lines. The two sets of data were from plants grown in Beijing and Hainan, respectively. Different letters above each column indicate significant difference ($P < 0.05$) between the two compared values. For all the data, each data point is derived from 30 individual plants, and bars indicate SD. One asterisk indicates significant difference ($P < 0.05$), and two asterisks indicate extremely significant difference ($P < 0.01$) in comparison with the corresponding wild-type value.

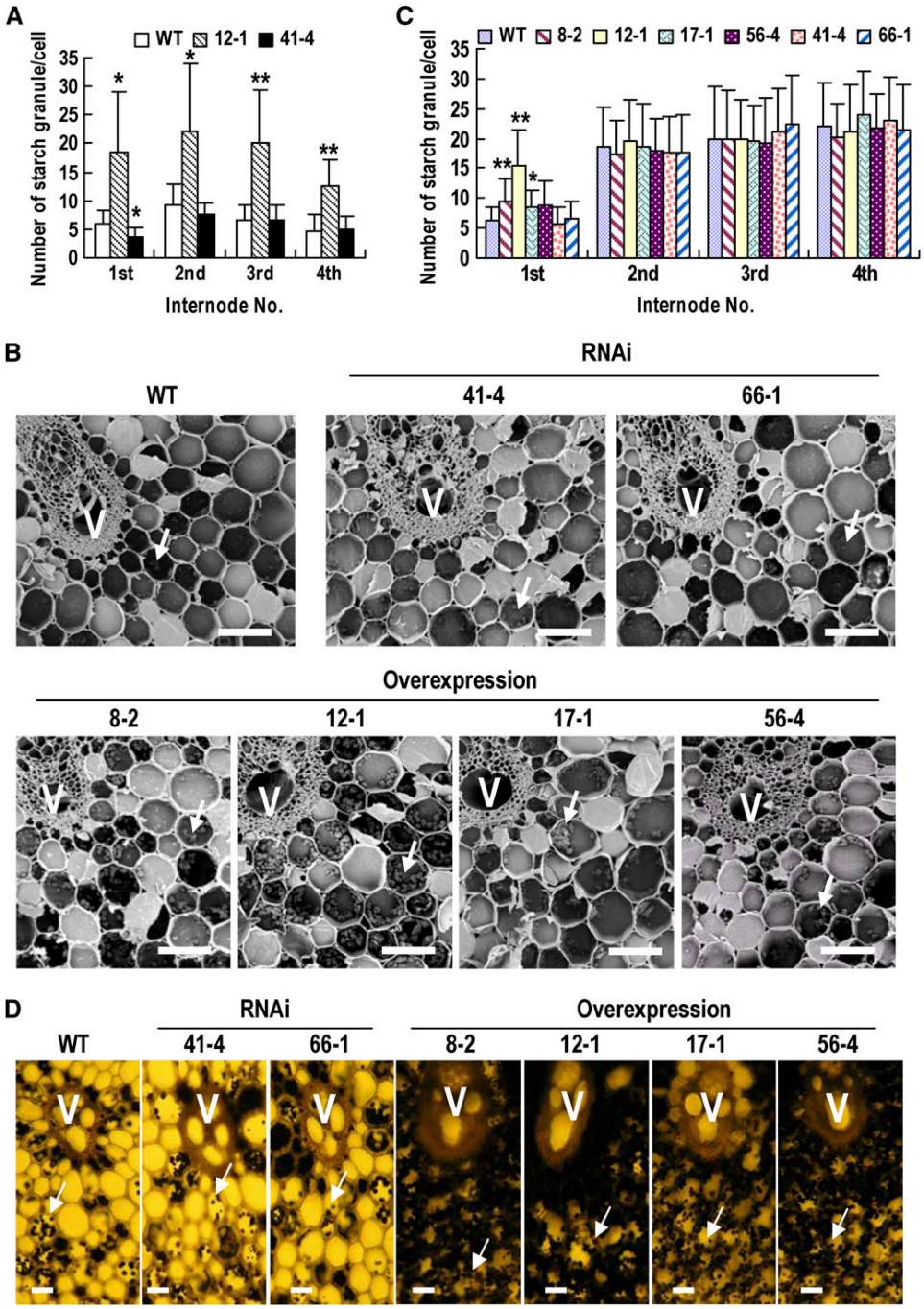

Figure 6. Starch Accumulation in the Internodes of the *ETR2* Transgenic Plants.

(A) Number of starch granules in the *ETR2*-overexpressing line 12-1, the RNAi line 41-4, and control plants that have identical growing time. All plants are at the ripening stage. For each line, four internodes from the top to bottom were cross-sectioned, and sections were examined for starch granules by scanning electron microscopy. Data are the average numbers from 30 cells. Bars indicate SD.

(B) Scanning electron micrograph of the cross sections from the first internode of the *ETR2*-overexpressing plants, the RNAi plants, and the control plants. These plants are at the same developmental stage after heading but have different growing times. V indicates vascular tissue and an arrow indicates a starch granule. Bars = 40 μM.

(C) The number of the starch granules in the transgenic and control plants that are at the same developmental stage after heading. Data are the average numbers from 30 cells as in the sections from **(B)**. Bars indicate SD.

(D) Iodine staining of starch granules from the first internode of the transgenic and control plants that are at the same developmental stage after heading but have different growing times. Other indications are the same as in **(B)**. One asterisk indicates significant difference ($P < 0.05$), and two asteriaks indicate extremely significant difference ($P < 0.01$) in comparison with the corresponding wild-type value.

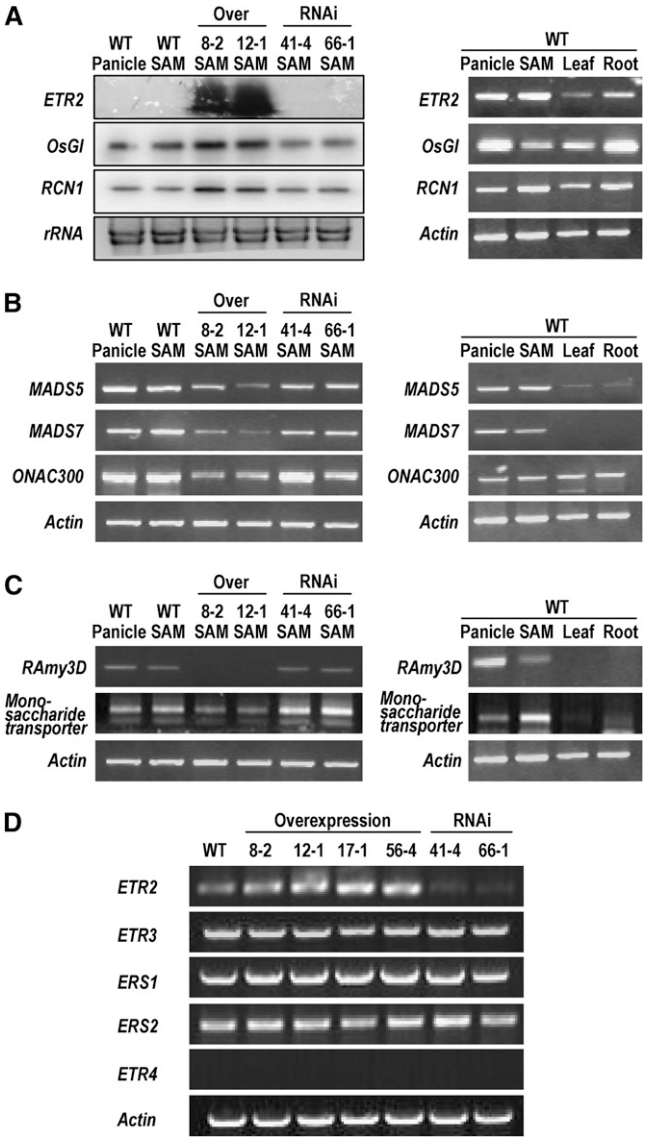

Figure 7. Altered Gene Expression in *ETR2*-Overexpressing Plants and RNAi Plants.

(A) Genes upregulated by *ETR2*. Total RNAs were isolated from the SAM and other organs. In the left panel, total RNAs were subjected to RNA gel blot analysis using probes synthesized from the *ETR2*, *OsGI*, and *RCN1* genes, respectively. The RNA loading was examined by ethidium bromide staining. "Over" indicates *ETR2*-overexpressing lines, and "RNAi" indicates the RNAi lines. In the right panel, the total RNAs from different organs of the control plants (WT) were subjected to RT-PCR analysis. The rice *Actin* gene was amplified as a control.

(B) Genes downregulated by *ETR2*. RT-PCR was performed to examine the expression of the *MADS5*, *MADS7*, and *ONAC300* genes in the transgenic and control plants. The *Actin* gene was amplified as a control.

(C) The α-amylase gene and a monosaccharide transporter gene are downregulated by *ETR2*. The two genes were examined by RT-PCR in the transgenic and control plants. The *Actin* gene was amplified as a control.

(D) Expression of the five ethylene receptor genes in *ETR2*-overexpressing plants and the RNAi plants. For all RT-PCR analyses, three biological replicates were performed, and the results were consistent. One set of the results is shown.

ethylene receptor genes were observed in these rice seedlings (Figure 7D).

Identification and Phenotypic Comparison of T-DNA Insertion Mutants for *ETR2* and Other Ethylene Receptor Genes

To further investigate ETR2 function, the T-DNA insertion mutant, *etr2*, for the *ETR2* gene was requested from the Rice Mutant Database (http://rmd.ncpgr.cn) and analyzed. For comparison, the T-DNA insertion mutant *etr3* and *ers2* for rice *ETR3* and *ERS2*, respectively, were also studied. These mutants were in the background of Zhong Hua 11 (ZH), a *japonica* variety. In *etr2*, the T-DNA was inserted at 0.6 kb upstream of the ATG start codon of *ETR2* gene (Figure 8A). In *etr3*, the insertion was found at 0.9 kb upstream of the *ETR3* start codon. In *ers2*, the insertion was at 0.7 kb downstream of the *ERS2* stop codon. Homozygous lines of these mutants were identified (Figure 8A). In *etr2*, *ETR2* expression was barely detectable; however, in *etr3* or *ers2*, *ETR3* or *ERS2* was still expressed at low levels (Figure 8B). Thus, *etr2* appeared to be a near-knockout mutant, whereas *etr3* and *ers2* were knockdown mutants.

The three T-DNA insertion mutants were treated with ethylene, and their coleoptile growth response was examined. The *etr2* mutant exhibited the longest coleoptile at all ethylene concentrations tested compared with controls (Figure 8C). The *etr3* and *ers2* mutants showed moderate length of coleoptiles with these treatments compared with controls (Figure 8C). These results indicate that the three mutants have an enhanced ethylene response, suggesting that reduction of ethylene receptor gene expression results in increased ethylene sensitivity.

The mutants were grown under field conditions to observe the effect of reducing expression of the receptor. We found that *etr2* and *etr3* developed panicles earlier than ZH control plants (Figure 9A). During the heading period, *etr2* and *etr3* plants showed early heading panicles compared with ZH controls (Figure 9B). The heading time distribution of these mutants was also analyzed. The *etr2* mutant showed a 3-d early heading, whereas the *etr3* had a 7-d early heading compared with ZH control plants (Figure 9C). These results indicate that reduction of ethylene receptor gene expression leads to early flowering.

Since overexpression of *ETR2* causes starch accumulation in stems (Figure 6), we examined whether reduction of *ETR2* and *ETR3* gene expression would affect starch accumulation. In both the *etr2* and *etr3* mutants, starch granules were almost absent in stems (Figure 9D). However, in the ZH control, starch granules were still abundant (Figure 9D). These results indicate that reduction of ethylene receptor gene expression causes disappearance of starch granules.

The seed phenotypes were compared, and the *etr2* and *etr3* mutant seeds appeared slightly larger than those of the ZH controls and *ers2* (Figure 9E). The thousand-seed weight was also examined, and *etr2* seeds had significantly higher thousand-seed weight than ZH control (Figure 9E). However, *etr3* seeds and *ers2* seeds had slightly higher and lower levels of the parameter, respectively, than the ZH control (Figure 9E). These analyses indicate that reduction of *ETR2* expression leads to high

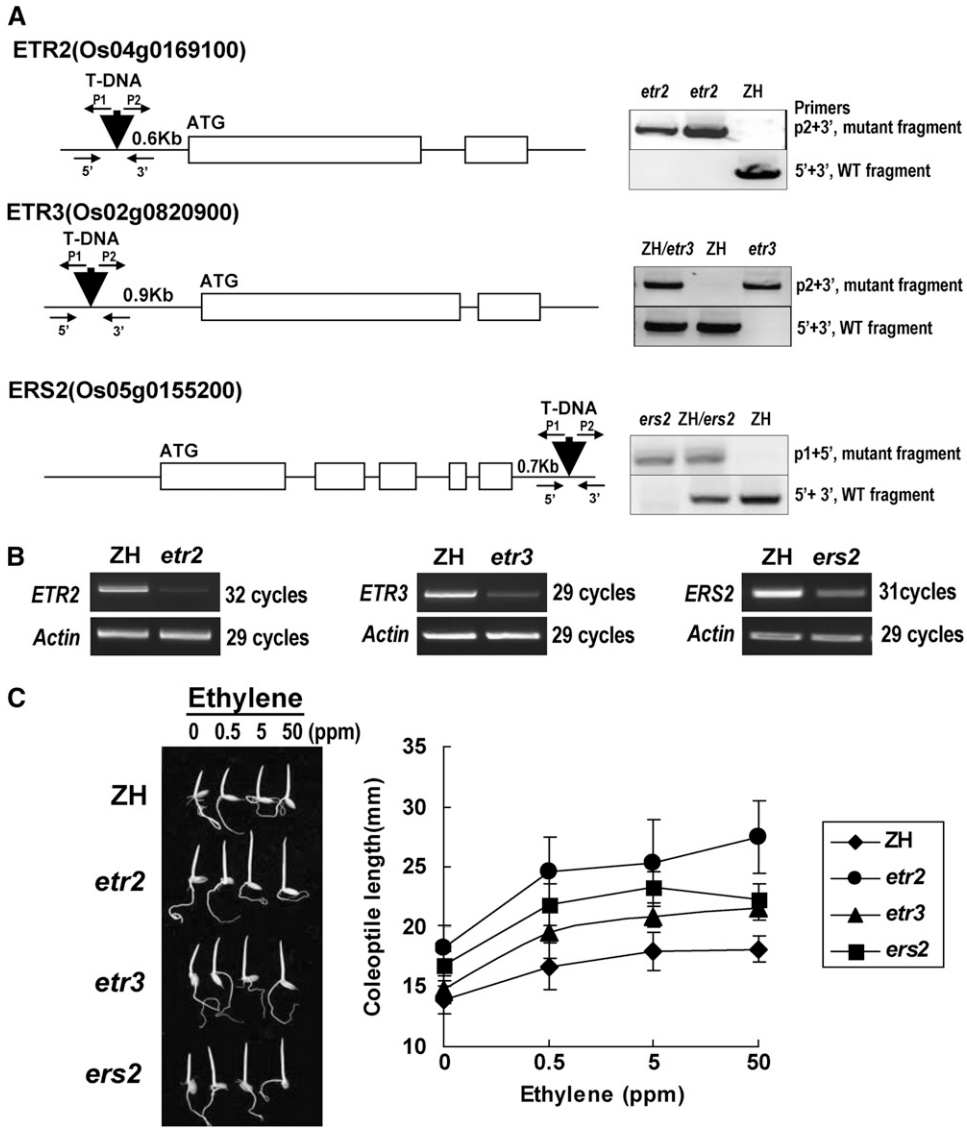

Figure 8. Identification of T-DNA Insertion Mutants and Their Ethylene Sensitivity.

(A) Schematic representation of T-DNA insertions in *ETR2*, *ETR3*, and *ERS2* genomic sequences and PCR identification of mutants. The *etr2*, *etr3*, and *ers2* are mutant plants for *ETR2*, *ETR3*, and *ERS2*, respectively. ZH (Zhong Hua 11) is the parental control plant. ZH/*etr3* and ZH/*ers2* are heterozygous plants. p1 and p2 are primers from the T-DNA regions. The 5′- and 3′-primers are from the genes examined. ATG indicates the start codon.
(B) Examination of *ETR2*, *ETR3*, and *ERS2* expression in their corresponding mutants by RT-PCR. *Actin* was amplified as a control. Three biological replicates for RT-PCR were performed, and the results were consistent. One set of the results is shown.
(C) Coleoptile growth of *etr2*, *etr3*, and *ers2* in response to ethylene treatment. Left panel: phenotype of the etiolated seedlings after ethylene treatment. Right panel: coleoptile growth of various mutants after ethylene treatments. Each data point represents the average of 20 to 30 seedlings. Bars indicate SD.

thousand-seed weight. However, suppression of *ETR3* and *ERS2* results in more or less variation than ZH control in this parameter.

Since overexpression of *ETR2* causes an increase of *OsGI* and *RCN1* expression, but a decrease of *RAmy3D* and monosaccharide transporter gene expression (Figures 7A and 7C), we examined whether these genes were altered in the SAM of the three mutant rice plants. Both *OsGI* and *RCN1* expression were reduced in the three mutants compared with the ZH controls (Figure 9F). By contrast, *RAmy3D* and monosaccharide transporter gene expression were upregulated in the three mutants compared with the ZH control (Figure 9F). The expression of the above genes in the *etr2* mutant was consistent with that in the *ETR2*-overexpressing lines but not in the *ETR2*-RNAi lines

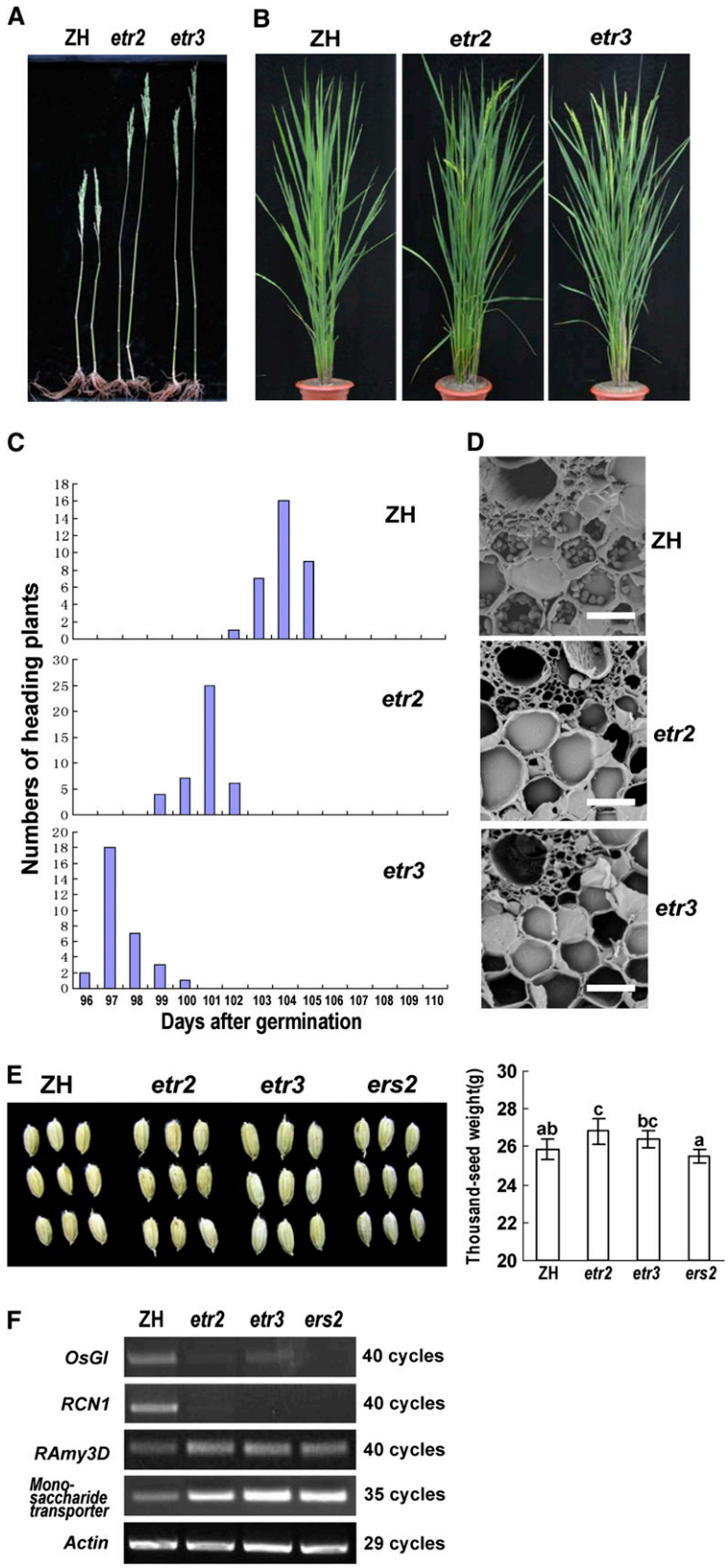

Figure 9. Phenotype of *etr2* and *etr3* Mutants in Comparison with the Control ZH (Zhong Hua 11).

(Figures 7A and 7C), probably because the *ETR2*-RNAi lines had a partial reduction but not an elimination of *ETR2* expression. These results indicate that suppression of ethylene receptor gene expression in T-DNA insertion mutants leads to inhibition of *OsGI* and *RCN1* but upregulation of *RAmy3D* and the monosaccharide transporter gene.

DISCUSSION

We have studied the ethylene receptor from the monocotyledonous rice plant and found that subfamily II ethylene receptor ETR2 is a Ser/Thr kinase that can phosphorylate its own receiver domain and an in vitro substrate MBP. Complete abolishment of ETR2 kinase activity by N box mutation suggests that the N box is the most important motif for ETR2 function (Figure 2). Overexpression of *ETR2* leads to reduced ethylene sensitivity and late flowering, whereas T-DNA insertion mutant *etr2* showed enhanced ethylene sensitivity and early flowering (Figures 3, 4, 8, and 9). Other yield-related traits, starch accumulation, and gene expressions were also affected by *ETR2* overexpression or reduction (Figures 5 to 7). This study reveals conserved and diverged aspects in ethylene receptor signaling between the monocotyledous rice plant and dicotyledonous plant.

While Ser/Thr kinase activity has been found in subfamily II receptors from dicotyledonous plants (Xie et al., 2003; Moussatche and Klee, 2004; Zhang et al., 2004), we show here that ETR2, from a monocotyledonous plant rice, possesses Ser/Thr kinase activity. Mutations in the N box of NTHK2 and *Arabidopsis* receptors partially reduced their kinase activities (Moussatche and Klee, 2004; Zhang et al., 2004). However, the rice ethylene receptor ETR2 completely lost its kinase activity through mutation of the N box. This property demonstrates that the Ser/Thr kinase activity of ETR2 is intrinsic and not from other contaminating proteins, which might be questioned during analysis of yeast-expressed proteins. This feature may reflect the further divergence of the rice ethylene receptors in terms of structure and function, or it could have resulted from mutations of different amino acid residues. The phosphorylation sites in ETR2 are likely in the ATP subdomain, since the truncated form without the ATP subdomain fails to be phosphorylated by ETR2. In the tobacco ethylene receptor NTHK1, the phosphorylation sites are mainly located in the HIS and ATP subdomains (Zhou et al., 2006a). ETR2 can phosphorylate its RD. This property was not found for NTHK1, NTHK2, and *Arabidopsis* receptors (Xie et al., 2003; Moussatche and Klee, 2004; Zhang et al., 2004). However, whether and how the RD phosphorylation would mediate the receptor signal output needs to be further studied.

Although ethylene receptors have kinase activities, the physiological function of these activities is largely unknown and of uncertain significance. Histidine kinase activity of *Arabidopsis* ETR1 may have no role or might be involved in growth recovery or ethylene-independent growth regulation (Wang et al., 2003; Binder et al., 2004; Qu and Schaller, 2004; Cho and Yoo, 2007). The Ser/Thr kinase activity of tobacco NTHK1 appeared to be required for plant leaf growth and stress responses (Chen, 2008). However, the role of ETR2 Ser/Thr kinase activity in rice ethylene signaling needs to be investigated. It is possible that the Ser/Thr kinase activity of the ethylene receptor could phosphorylate its interacting proteins and then transfer the signal to downstream components. Identification of these interacting proteins should shed light on the mechanism of receptor signal transduction in the future.

Rice plants have at least five ethylene receptors. However, among these, no ETR1-like receptor (i.e., subfamily I receptor with a receiver domain) was identified after analysis of the whole rice genome. This is in contrast with the observation that dicotyledonous plants generally have ETR1-like proteins. Pareek et al. (2006) have analyzed the rice genome for two-component signaling machinery but did not identify an ETR1-like receptor. These results possibly imply that rice may not have an ETR1-like protein. However, rice does contain subfamily I receptors, ERS1 and ERS2, neither of which contains a receiver domain. Gallie and Young (2004) have analyzed ethylene perception machinery in maize and they failed to identify an *ETR1*-like gene, although they were able to isolate other ethylene receptor genes. The significance of the absence of an ETR1-like protein in monocotyledonous cereal plants remains to be studied.

Overexpression of the *ETR2* gene conferred reduced ethylene sensitivity in rice plants, whereas the *etr2* mutant showed enhanced ethylene sensitivity (Figures 3 and 8). The T-DNA insertion mutants *etr3* and *ers2*, with reduced expression of *ETR3* and *ERS2*, respectively, also had increased ethylene sensitivity (Figure

Figure 9. (continued).

(A) Panicle development in mutants and the control line ZH. Tillers from field-grown rice plants (98 d) were peeled, and the two most developed panicles are shown.

(B) Heading of mutants and control line ZH. Plants (100 d) were carefully pulled out from the field and regrown in pots for photography.

(C) Heading time distribution of the mutants and control line ZH. During the heading period, the number of the heading plants for mutants and the control line grown in the field was recorded each day and analyzed.

(D) Comparison of starch granules in cross sections from the first internode of mutants and control plants. Plants (119 d) during the grain-filling period were used for cross section and observation under a scanning electron microscope. Bars = 40 μM.

(E) Comparison of seed phenotype (left panel) and thousand-seed weight (right panel). Seeds from *etr2*, *etr3*, *ers2*, and the control line ZH were compared. Different letters above each column indicate significant difference ($P < 0.05$) between the two compared values.

(F) Altered gene expression in rice mutants and control line. The late-flowering gene *OsGI* and *RCN1*, α-amylase gene *RAmy3D*, and a monosaccharide transporter gene were examined by RT-PCR. *Actin* gene was amplified as a control. Three biological replicates for RT-PCR were performed and the results were consistent. One set of the results is shown.

8). This observation was in line with the roles of the ethylene receptor NTHK1 in tobacco and *Arabidopsis* (Xie et al., 2002; Cao et al., 2007). Consistently, overexpression of the tomato ethylene receptor *NR* reduced ethylene sensitivity in seedlings and mature plants, whereas transgenic plants with reduced tomato *ETR4* gene expression exhibited multiple symptoms of extreme ethylene sensitivity (Ciardi et al., 2000; Tieman et al., 2000). Although both the shoots and roots of rice are responsive to ethylene or ACC treatment, their responses are different: root growth was suppressed, whereas coleoptile growth was promoted. The etiolated rice seedlings did not have a typical triple response as *Arabidopsis* or other dicotyledonous plants do upon ethylene treatment. This phenomenon represented a special feature for rice seedlings due to difference in seedling structures from dicotyledonous plants. Dicotyledonous seedlings have two cotyledons and a long hypocotyl when grown in the dark, whereas etiolated rice seedlings have only very short mesocotyls (Maclean et al., 2002). Further studies should reveal how ethylene signaling could exert different effects on root and shoot growth.

ETR2 can delay floral transition, and this was supported by the results from overexpression, RNAi, and T-DNA insertion mutant analysis (Figures 4 and 9). An abundance of *ETR2* transcripts in the SAM and panicle (Figure 7A) further supports this conclusion. Consistently, the T-DNA insertion mutant *etr3* for another rice ethylene receptor gene *ETR3* showed early flowering (Figure 8). The tobacco ethylene receptor NTHK1 also caused a late flowering phenotype in transgenic *Arabidopsis* (Cao et al., 2007). Similarly, the *Arabidopsis* gain-of-function mutant *etr1-1* of ethylene receptor ETR1 displayed late flowering (Bleecker et al., 1988; Ogawara et al., 2003). An ethylene receptor gain-of-function mutant in tomato, *NR* (never ripe), originally identified by its lack of fruit ripening, exhibited delayed flower development (Lanahan et al., 1994). Since ethylene negatively regulates its receptors (Hua and Meyerowitz, 1998), ethylene should promote plant flowering through suppression of ethylene receptor functions. It has been reported that ethylene induced flowering in pineapple (*Ananas comosus*) and that silencing of the ACC synthase gene caused delayed flowering in pineapple (Abeles et al., 1992; Trusov and Botella, 2006). In addition to ethylene receptors, other components of ethylene signaling also affect flowering time. Ethylene-insensitive mutants *ein2-1* and *ein3-1* and the constitutive ethylene response mutant *ctr1-1* showed a late flowering phenotype (Ogawara et al., 2003; Achard et al., 2007). Although ethylene can enhance floral development, it also inhibits flowering in some plant species (Abeles, 1967). Further studies should disclose the mechanism by which ethylene differentially regulates flowering in different plant species.

Microarray analysis of gene expression profiles in *ETR2*-overexpressing plants and *ETR2*-RNAi plants revealed that ETR2 affected flower development (see Supplemental Figures 1 and 4 online). Two flowering-related genes *OsGI* and *RCN1* were consistently upregulated in *ETR2*-overexpressing plants but downregulated in the *etr2* mutant. These two genes were also suppressed in *etr3* and *ers2* mutants (Figure 9). It has been reported that overexpression of *OsGI* caused late flowering in transgenic rice, and this function was likely due to the activation of the *CONSTANS* homolog *Heading date1* (*Hd1*) and suppression of the *FLOWERING LOCUS* (*FT*) homolog *Hd3a* (Hayama et al., 2003). The *Arabidopsis FT* homolog *TERMINAL FLOWER1*/*CENTRORADTALIS* (*TFL1*/*CEN*) gene retards floral transition (Kobayashi et al., 1999), and *RCN1*, the rice homolog of *TFL1*/*CEN*, was also found to cause delayed transition from vegetative to reproductive development in the SAM of transgenic rice (Nakagawa et al., 2002). It is thus proposed that ETR2 may delay floral transition at least partially through activation of the *OsGI-RCN1* pathway. However, it is not known whether the regulation of floral transition by ETR2 is through the CTR1-EIN2-EIN3–mediated ethylene response pathway or whether ETR2 has a role in flowering time that is distinct from its role in ethylene signaling. Further studies should test these possibilities.

ETR2 promoted starch accumulation in plant internodes (Figure 6), and this accumulation was possibly due to the reduced expression of the *RAmy3D* gene, whose product, α-amylase, hydrolyzes starch. A monosaccharide transporter gene was also suppressed in the *ETR2* overexpression lines, and this suppression may prevent sugar translocation from the stem to grains, leading to reduced seed-setting rate and reduced thousand-seed weight (Figure 5). When expression of *ETR2* was reduced in the *etr2* mutant and/or RNAi lines, starch failed to accumulate, and sugar translocation was enhanced, resulting in higher thousand-seed weight (Figures 5, 6, and 9). Parameters from a different year also support this conclusion (see Supplemental Figure 7 online). Inhibition of *RAmy3D* by ETR2 in this study may be consistent with a report showing that ethylene induced *RAmy3D* gene expression in rice (Fukao et al., 2006). Under submergence in water, the intolerant rice cultivar M202 produces more ethylene than tolerant M202(Sub1) plants and has decreased starch content. This process of starch metabolism was also regulated by the ERF-type transcription factor Sub1C (Fukao et al., 2006). Ethylene, together with abscisic acid, also had an influence on grain filling (Yang et al., 2006). These studies imply that ethylene and receptor signaling can regulate carbohydrate metabolism, sugar translocation, and grain filling in rice. The mechanism reported here provides significant clues for improvement of yield-related traits in rice. It should be noted that although reduction of *ETR2* expression could increase thousand-seed weight, suppression of ethylene receptor genes *ETR3* and *ERS2* in their corresponding mutants only slightly changed this parameter. However, the *etr3* mutant seeds appeared larger than the other seeds evaluated (Figure 9E). These observations suggest that each ethylene receptor gene may regulate specific seed-related traits.

Arabidopsis GI affected both floral initiation and starch accumulation (Araki and Komeda, 1993; Eimert et al., 1995). We therefore speculate that the rice ethylene receptor ETR2 may regulate floral transition and starch accumulation partially by regulating the *OsGI* gene. Another *cam1* mutant of *Arabidopsis* also had delayed floral initiation and altered starch metabolism. However, not all the late-flowering mutants had increased starch content, and the higher starch level is not the cause of the late floral transition (Eimert et al., 1995). It is possible that starch accumulation and floral transition share a common signaling pathway. Alternatively, plants may use the OsETR2-OsGI pathway to store energy and use it later for reproduction, once the ethylene signal is available for receptor inhibition at a proper time or appropriate developmental stage.

METHODS

Plant Materials and Growth Conditions

Japonica rice (*Oryza sativa*) variety Taipei 309 (TP309) and Zhong Hua 11 (ZH) were used in this study. Rice seeds from control plants, *OsETR2*-overexpressing plants, *OsETR2*-RNAi transgenic plants, or T-DNA insertion mutants were immersed in water for 2 d and grown for ~45 d in soil seed bed, and then the seedlings were transplanted to the field. The field was located in the Experimental Station of the Institute of Genetics and Developmental Biology, Chinese Academy of Sciences (39°48'N, 116°28'E). The growing season is from the end of April to the end of October. During this period, the average lowest temperature is from ~7 to ~22°C, and the average highest temperature is from ~19 to ~31°C. The light period of the photoperiod is from ~7.2 to ~9.3 h. The plants were maintained following routine management.

Cloning of the *ETR2* Genomic and cDNA Sequences

The rice *ETR2* genomic sequence was amplified from genomic DNA using the primers 5′- GAAAGATCTATGCCACCGATCCCATCTCTG-3′ and 5′-CAAGGTACCTGTGATTGTATGGACCTAAC-3′. The amplified fragment was cloned into the T-easy vector and sequenced, and the position of its intron was determined by comparison with the cloned 3′-cDNA sequence spanning the intron region. The primers 5′-CATGGTAGGTACTCTAATAC-3′ and 5′-CAAGGTACCTGTGATTGTATGGACCTAAC-3′ were used to amplify the 3′-cDNA of *ETR2*. The full-length coding-region of *ETR2* was also amplified from the first-strand cDNAs derived from the total RNAs of rice seedlings, cloned into a T-easy vector and used for further analysis.

Expression of the Truncated ETR2 Proteins

For expression of different truncated versions of ETR2 as GST fusions in *Escherichia coli*, the pGEX4T-1 vector was used. DNA fragments corresponding to the putative kinase domain (wild type, amino acids 180 to 619), the kinase domain without the ATP binding motif (ΔATP, amino acids 180 to 461), and the putative RD (amino acids 631 to 756) were amplified from the original rice *ETR2* cDNA. For the wild type, the sense primer is OsETR2-KD-LEFT (5′-CGGGATCCATGCTCACGCACGAGATC-3′) and the antisense primer is OsETR2-KD-RIGHT (5′-ACGCGTCGACGAGTCACATGCTGCAGCT-3′). For ΔATP, the sense primer is the same as that for the wild type, and the antisense primer is OsETR2-KD (ΔATP)-RIGHT (5′-ACGCGTCGACCAACACTGATTGCCTCCT-3′). The primers for RD are OsETR2-RD-LEFT (5′-CGGGATCCGTCTCTGGAGCATCCTCG-3′) and OsETR2-RD-RIGHT (5′-ACGCGTCGACACAGTTCATCTCCCAGTG-3′). The multisite mutations in the N box (N, with mutations G487A, E489Q, R491Q, F493A, and G501A) were made through the overlapping PCR method by the Shanghai Sangon Company, and the mutation was confirmed by sequencing. Finally, the PCR products for the wild type, ΔATP, N, and RD were digested with *Bam*HI/*Sal*I, cloned into the *E. coli* expression vector pGEX4T-1, and confirmed by sequencing. The recombinant plasmids were transformed into *E. coli* strain BL21. The positive colony was grown in 5 mL 2× Yeast Extract Tryptone medium at 37°C for 12 h, and the cultured cells were transferred into 100 mL 2× Yeast Extract Tryptone medium and grown for 10 h at 37°C.The expression of recombinant proteins was induced by addition of isopropyl-β-D-thiogalactopyranoside to a concentration of 400 μM and grown at 30°C for 2.5 h. After induction, the *E. coli* cells were broken by sonication in 10 mL extraction buffer (50 mM Tris-HCl, pH 7.6, 100 mM NaCl, 1 mM EDTA, and 10% [v/v] glycerol), and the supernatant was loaded onto the GST affinity resin in the column. The resin was washed extensively with washing buffer (50 mM Tris-HCl, pH 7.7, 100 mM NaCl, 0.1% [v/v] Tween 20, and 10% [v/v] glycerol) and finally eluted for GST fusion proteins with elution buffer (10 mM reduced glutathione and 50 mM Tris-HCl, pH 8.0) (Xie et al., 2003; Zhang et al., 2004). The free glutathione was removed on a centriprep concentrator, and the buffer was changed to storage buffer (50 mM Tris-HCl, pH 7.6, 50 mM KCl, 2 mM DTT, and 10% [v/v] glycerol). The expression and purification of the GST fusion proteins were confirmed by protein gel blotting using a mouse anti-GST monoclonal antibody (Amersham). The GST protein itself was also expressed and used as a control.

Kinase Assay

The purified GST fusion proteins were examined for their kinase activity, and GST was used as a control. Phosphorylation was performed in 25 μL of assay buffer (50 mM Tris–HCl, pH 7.6, 50 mM KCl, 2 mM DTT, 10 μM ATP, and 10% [v/v] glycerol) containing 1 μg GST fusion proteins in the presence of 5 mM of $MnCl_2$, $MgCl_2$, or $CaCl_2$. The phosphorylation was initiated by adding 25 μCi of [γ-^{32}P] ATP (5000 Ci mmol^{-1}) and incubated at 22°C for 45 min (Xie et al., 2003; Zhang et al., 2004). The phosphorylated proteins were subjected to 10% SDS-PAGE and transferred onto PVDF membranes (Amersham). The incorporated phosphate was visualized by autoradiography. Coomassie Brilliant Blue staining of the same membrane was also performed to verify the protein loading. The stability of the incorporated phosphate was determined by treating the membranes with water, 1 M HCl, or 3 M NaOH for 2 h to overnight at room temperature. The treated membranes were then subjected to autoradiography. For substrate phosphorylation, wild-type or N protein was incubated under phosphorylating conditions with no substrate or with MBP, ΔATP, RD, or GST. The phosphorylated proteins were resolved on an SDS-PAGE gel, transferred to PVDF membranes, and subjected to autoradiography or Coomassie Brilliant Blue staining.

Phosphoamino acid analysis followed previous descriptions (Xie et al., 2003).

Generation of Transgenic Rice Plants

The genomic DNA sequence of the *ETR2* gene, which contains a 370-bp intron, was cloned into the *Bam*HI/*Kpn*I sites of the pBIN438 binary vector, between the cauliflower 35S promoter and nopaline synthase (nos) terminator, to generate the pBIN438-OsETR2 construct for overexpression analysis. The primers used to amplify this insert were 5′- GAAAGATCTATGCCACCGATCCCATCTCTG-3′ and 5′-CAAGGTACCTGTGATTGTATGGACCTAAC-3′. The tobacco mosaic virus sequence was included downstream of the double 35S promoter to enhance the translation efficiency. For the RNAi construct, primers R1 (5′-CACTCTAGAGAGCTCAGAGCAAAGCATGAAACCACG-3′) and R2 (5′- CGCGTCGACGGTACCACAGCCTGCATTACACCTCTG-3′) were used for amplification of the 433-bp *ETR2* fragment (from positions 1100 to 1533 bp). This fragment was inserted into the pZH01 binary vector in an inversely oriented manner, and with a β-glucuronidase fragment in between the two inserted fragments, to generate the RNAi construct pZH01-OsETR2-RNAi. The fused gene was under the control of the cauliflower 35S promoter. Transgenic rice plants were generated according to *Agrobacterium tumefaciens*–mediated transformation methods described by Zhou et al. (2006b). Briefly, the coat-stripped TP309 seeds were sterilized in 20% NaClO solution, washed with sterilized water three times, and plated on NB medium [N6 salts and B5 vitamins, supplemented with 30 g/l maltose, 500 mg/l proline, 300 mg/l casein hydrolate, 500 mg/l glutamine, and 2 mg/l 2,4-D (pH 5.8)]. The scutellum-driven embryonic calli were induced from TP309 seeds after 1 to 2 months. The calli were incubated with the *A. tumefaciens* strain AGL1, carrying the overexpression or RNAi plasmids, at room temperature for 20 to 30 min and then cocultured on NB medium containing 0.1 μM

acetosyringone for 2 d. For selection of positive *OsETR2*-overexpressing transformants, the calli were transferred to NB medium containing 80 mg/L G-418 and 500 mg/L cefotaxime, maintained for 3 weeks at room temperature, and then transferred to NB medium containing 150 mg/L G-418 and 500 mg/L cefotaxime, and maintained for another 3 weeks. For selection of RNAi transformants, 50 mg/L hygromycin was used. After selection, the calli were transferred to Shoot Regeneration medium for shoot regeneration and the medium (half-strength Murashige and Skoog salts containing 0.5 mg/L napthalene acetic acid) for root development. The transgenic plants were then transferred to the field of the Experimental Station (Institute of Genetics and Developmental Biology, Chinese Academy of Sciences) for normal growth and seed harvesting.

Measurement of Agronomic Traits and Material Collection

Seeds of control and T2 or T3 homozygous transgenic plants were soaked in water for 3 d at 37°C and then transferred to Petri dishes with wet cheesecloth at 28°C. Elongation of the shoot was measured at 5-d intervals. The seedling length was also measured for the 50-d-old seedling grown in the field. Flower development was observed at ~100 d after germination and then the heading date of each transgenic line, controls (TP309 and Zhong Hua 11) or mutants were examined every day. Plant height and internode length were measured at the mature stage. The ratio of effective tillers, ratio of effective panicles, seed-setting rate, and thousand-seed weight were analyzed when the seeds were harvested. Effective tillers were defined as the tillers that have panicles, and the ratio of the effective tiller number to the total tiller number was regarded as the ratio of effective tillers. Effective panicles were defined as the panicles that have at least one full-sized grain, and the ratio of the effective panicle number to the total tiller number was regarded as the ratio of effective panicle. Seed-setting rate was defined as the ratio of full-size grain number to the total grain number. For each line, data from 30 individual plants were obtained and subjected to statistic analysis. For examination of gene expression, the roots and leaves were harvested from seedlings grown in water for 14 d. The SAM and panicles were collected from TP309 or transgenic rice plants grown in the field for 95 and 100 d after sowing, respectively. The materials were frozen in liquid nitrogen and stored at −80°C until extraction of DNA or RNA.

Isolation of Nucleic Acids and Hybridization Analysis

Total RNA isolation and RNA gel blot hybridization were performed following the description by Zhang et al. (1996, 1999b). Full-length rice *ETR2* cDNA was used as the template for probe labeling. For detection of *OsGI* expression, a 1005-bp fragment (from 1720 to 2725 bp in the open reading frame) was amplified with the primers 5′-CCTGTGCTTCAATGGACCTT-3′ and 5′-GCCAGAGCAATGAGACAACA-3′. For the detection of *RCN1*, a 646-bp fragment (from 177 to 823 bp in the open reading frame) was amplified using the primers 5′-TGACCTGCGATCTTTCTTCA-3′ and 5′-CACCAGCATGAATTGGCTTA-3′. Genomic DNA from rice leaves was isolated by an extraction method with SDS (Chen et al., 1991). Genomic DNA (8 μg) was digested with *Dra*I, resolved on a 0.8% (w/v) agarose gel, transferred to a nylon membrane, and hybridized using the labeled probes (Chen et al., 1991).

Determination of Ethylene Sensitivity

Rice seeds were immersed in water at 37°C for 2 d, transferred onto a plate containing wet cheesecloth, and grown at 28°C for another 3 d. The germinated seeds were then subjected to treatments with various concentrations of ACC (0, 10 nM, 100 nM, 1 μM, 10 μM, and 100 μM) in the dark. After 1 week, the lengths of the shoots and roots were measured. The experiment was repeated independently three times, and the results were consistent. For ethylene treatment, germinating seeds were transferred into 4-cm Petri dishes (20 per dish) fitted with eight layers of moist gauze. The Petri dishes were placed in air-tight plastic boxes (41 × 31.5 × 15 cm), which was used for reducing the effect of endogenous ethylene. Ethylene gas was injected into the plastic boxes using a syringe. Seed transfer and ethylene treatment were performed under dim green light as described by Ku et al. (1970). Seedlings were grown in darkness at 25°C. Coleoptile length was measured 3 d after ethylene treatment.

Starch Analysis

Premature rice stems were collected and used for scanning electron microscopy analysis. For the same growth stage experiment, 162-d-old field-grown control TP309, overexpression line 12-1, and RNAi line 41-4 were used. For the same developmental stage experiment, the sampling days were varied for different lines. In detail, 123-d-old TP309, 120-d-old RNAi lines 41-4 and 66-1, 136-d-old overexpression lines 8-2, 17-1, and 56-4, and 150-d-old overexpression line 12-1 were used. The lower parts (adjacent to the nodes) of the first to fourth internodes were collected, and then the samples were cross-sectioned using a razor blade. The fixation, dehydration, and scanning electron microscopy observation followed the description by Cao et al. (2007). The starch numbers in 30 cells for each sample were calculated.

The cross sections were also subjected to iodine staining with 1% (w/v) KI solution to reveal the starch granules. The sections were washed with water and observed under a light microscope (Olympus U-25ND6).

Microarray Analysis

Two biological replicate samples of SAMs from *Japonica* control variety TP309 (95 d), the *ETR2*-overexpression line 12-1 (100 d), and the *ETR2*-RNAi line 41-4 (92 d) were collected for RNA extraction from field-grown rice plants. Each replicate contains 10 to 20 SAMs from ~10 individual rice plants grown in the same field. These SAMs were at the same vegetative stage but were grown for different periods of time. Plants were grown under field conditions with regular management, including irrigation and routine pest control. The total RNAs were extracted from each replicate using the RNeasy Mini Kit (Qiagen) and used in target synthesis for the Rice Genome Array from Affymetrix. The cDNA synthesis and cRNA preparation were performed according to standard protocols (Affymetrix). Hybridization, washing, and staining were conducted in an Affymetrix Genechip Hybridization Oven 640 and Affymetrix Fluidics Station 450. The scanning and data collection and analysis were performed using a Gene array Scanner 3000 7G and GeneChip Operating Software (Affymetrix). The rice genome array contains probes to query 51,279 transcripts representing two rice cultivars, with ~48,564 japonica transcripts and 1260 transcripts representing the indica cultivar. The entire analysis was performed at Shanghai Biochip Company and followed standard protocols from Affymetrix.

Examination of Gene Expression by RT-PCR Analysis

For RT-PCR analysis of the putative downstream genes, cDNA was reverse transcribed from the total RNAs of the SAM and used as templates for PCR amplification with specific primers for the selected genes. The PCR reactions were performed at 94°C for 50 s, 54 to 58°C for 60 s, and 72°C for 60 s for 30 cycles unless stated, and the products were visualized with ethidium bromide. For *Actin*, the primers are R-Actin A (5′-GGAACTGGTATGGTCAAGGC-3′) and R-Actin B (5′-AGTCTCATGGATAACCGCAG-3′); for *ETR2*, the primers are OsETR2-A (5′-CATGGTAGGTACTCTAATAC-3′) and OsETR2-B (5′-TGTGATTGTATGGACCTAAC-3′); for *MADS5*, the primers are 5′-GCGAGGGAAAGTAGAGCTGA-3′ and 5′-ACCCGCATGTAAAAGAGAGC-3′; for *MADS7*, the primers

are 5′-TGGAGCTGAAGAGGATCGAG-3′ and 5′-AATTCATTGTCCCCG-TCATC-3′; for *RAmy3D*, the primers are left primer (5′-CCCCTAAAATG-GAACGGGTA-3′) and right primer (5′-ACTGCATCCTGAACCTGACA-3′); for *ONAC300*, the primers are 5′- AGAACGGCATCTGCTACACC-3′ and 5′-ATATACCTGCCCTGCCCTCT-3′; and for the putative monosaccharide transporter, the primers are 5′-GTCATCGTCATCGCCTTCTT-3′ and 5′-AGGACAAACACGGGATGGTA-3′.

The primers for RT-PCR analysis of other rice ethylene receptor genes were as follows. For *ETR3*, 5′-TGAAGTTTGTCATTGGTGTC-3′ and 5′-CAGGATTCACAGCTTTTACC-3′ were used. For *ETR4*, 5′-TCAGGGT-GTCCATCTACGAC-3′ and 5′-TCCCATCTGAGAGGCTGGTAG-3′ were used. For *ERS1*, 5′-TGATAGCGCAAGAAATGGC-3′ and 5′-GTAAATA-CCTGAGGTAGATC-3′ were used. For *ERS2*, 5′-CGTGATCTACTAATG-GAGCA-3′ and 5′-ACATCTACCATCCATACATC-3′ were used.

Identification and Analysis of Rice T-DNA Insertion Mutants

The T-DNA insertion mutants and their parental variety Zhong Hua 11 (ZH) were requested from the Rice Mutant Database (http://rmd.ncpgr.cn). The *etr2*, *etr3*, and *ers2* mutant plants were identified using T-DNA primers p1 (5′-TGCAGGTTCTCTCCAAATGA-3′) and p2 (5′-AATCCA-GATCCCCCGAATTA-3′) and specific primers for the *ETR2*, *ETR3*, and *ERS2* genes as follows. For *etr2*, the 5′- and 3′-primers are 5′-ATC-GTGCAAATCTGCTCACT-3′ and 5′-CTCCTCCACAATCTGGCTCT-3′, respectively. For *etr3*, the 5′- and 3′-primers are 5′-CAATGACACTCAA-CCCACAA-3′ and 5′-CAAAGTGAATACAGGACGAA-3′, respectively. For *ers2*, the 5′- and 3′-primers are 5′-GGGAAGGAAGTTCGAGAAGG-3′ and 5′-TCAAGCGTATGAGCAAGCACC-3′, respectively. The receptor gene expression in these mutants was examined by RT-PCR with the primers described in the above section.

Determination of ethylene sensitivity, growing of the plants in the Experimental Station, observation and analysis of rice plant heading date, thousand-seed weight measurement, and downstream gene examination were all based on procedures in the above sections. For starch granules, cross sections of the first internodes holding panicles, which are from field-grown rice plants (119 d) during grain filling, were observed under a scanning electron microscope.

Statistical Analysis

All the data were analyzed by one-way analysis of variance with the program of SPSS (version 10.0). For the microarray data, the interquantile range (IQR) of each probe among all the six array hybridization results was calculated using R packages. Genes with a IQR value greater than the median IQR of all genes on the array (see Supplemental Figure 8 online) and that had a P value of <0.05 and a fold change greater than 1.8 between the transgenic line (*OsETR2*-overexpressing line 12-1 or the RNAi line 41-4) and TP309 were considered as differentially expressed genes (see Supplemental Data Sets 1 to 4 online). Multiple testing corrections (Benjamini and Hochberg false discovery rate) were used to adjust the P value. For the genes consistently regulated in both the *OsETR2*-overexpressing line 12-1 and the RNAi line 41-4 compared with the control line (see Supplemental Data Set 5 online), a fold change of 1.5 was considered to be significant. The selected genes in the text were further examined for their expression using RNA gel blot analysis or RT-PCR analysis. The internal control probes on the Affymetrix rice microarray exhibited no obvious changes between the RNAi/overexpression lines and the control lines.

The microarray data were further analyzed using the GOEAST program (Zheng and Wang, 2008; http://omicslab.genetics.ac.cn/GOEAST/index.php). The enriched Gene Ontology (GO) terms and their hierarchical relationships in biological process, cellular component, or molecular function GO categories were identified and provided as Supplemental Figures 1 to 6 online. The P value of GOID enrichment was calculated as the hypergeometric probability and resulted in so many probes/probe sets/genes for a GO term, under the null hypothesis, that they were picked out randomly from the microarray/genome. GOEAST by default adjusts the raw P values into false discovery rate using the Benjamini-Yekutieli method. False discovery rate is used for control of the type I error rate.

Accession Numbers

Sequence data from this article can be found in the GenBank/EMBL data libraries under the following accession numbers: Os ETR2/Os PK1, AF420319; Os ETR3/Os PK2, AF420318; Os ETR4/Os PK3, AF497626; Os GI, AK067038; RCN1, AF159882; MADS5, OSU78890; MADS7, OSU78891; RAmy3D, AA753608; ONAC300, AK102794; putative monosaccharide transporter, AK072059; and Zm ETR2, AB040406.

Supplemental Data

The following materials are available in the online version of this article.

Supplemental Figure 1. Biological Processes Affected in *ETR2*-Overexpressing Rice Line 12-1 Compared with Control Line TP309.

Supplemental Figure 2. Cellular Components Affected in *ETR2*-Overexpressing Rice Line 12-1 Compared with Control Line TP309.

Supplemental Figure 3. Molecular Functions Affected in *ETR2*-Overexpressing Line 12-1 Compared with Control Line TP309.

Supplemental Figure 4. Biological Processes Altered in *ETR2*-RNAi Rice Line 41-4 Compared with Control Line TP309.

Supplemental Figure 5. Cellular Components Affected in *ETR2*-RNAi Rice Line 41-4 Compared with Control Line TP309.

Supplemental Figure 6. Molecular Functions Affected in *ETR2*-RNAi Rice Line 41-4 Compared with Control Line TP309.

Supplemental Figure 7. Comparison of Seed-Setting Rate and Thousand-Seed Weight among *ETR2* Overexpression Lines, *ETR2*-RNAi Lines, and the Wild Type (TP309) Grown in a Year Different from Those in Figure 5.

Supplemental Figure 8. Plot of Gene Expression and IQR Values.

Supplemental Data Set 1. Genes Upregulated in *ETR2*-Overexpressing Rice Line 12-1 Compared with Control Line TP309.

Supplemental Data Set 2. Genes Downregulated in *ETR2*-Overexpressing Rice Line 12-1 Compared with Control Line TP309.

Supplemental Data Set 3. Genes Upregulated in *ETR2*-RNAi Rice Line 41-4 Compared with Control Line TP309.

Supplemental Data Set 4. Genes Downregulated in *ETR2*-RNAi Rice Line 41-4 Compared with Control Line TP309.

Supplemental Data Set 5. Genes Consistently Regulated in Both *ETR2*-Overexpressing Rice Line 12-1 and *ETR2*-RNAi Line 41-4 Compared with Control Line TP309.

Supplemental Data Set 6. Genes Selected for RT-PCR or RNA Gel Blot Analysis and Their Fold Changes in *ETR2*-Overexpressing Line 12-1 and *ETR2*-RNAi Line 41-4 Compared with Control Line TP309.

ACKNOWLEDGMENTS

We thank David Clark (University of Florida) for critical reading of the manuscript and Cheng-Cai Chu (Institute of Genetics and Developmental Biology, Chinese Academy of Sciences) for helpful comments. We also thank Qi Zheng and Jun Liu for their helpful discussions on

microarray analysis. We also thank the Rice Mutant Database (National Center of Plant Gene Research, Wuhan, at Huazhong Agricultural University) for providing rice mutant seeds. This work was supported by the National Natural Science Foundation of China (90717005), the National Basic Research Program of China (2006CB100102), the National Transgenic Research Project (2008ZX08009-003), and the High-Tech Program (2006AA10A101).

Received December 24, 2008; revised April 9, 2009; accepted April 21, 2009; published May 5, 2009.

REFERENCES

Abeles, F.B. (1967). Inhibition of flowering in *Xanthium pensylvanicum* Walln. by ethylene. Plant Physiol. **42:** 608–609.

Abeles, F.B., Morgan, P.W., and Saltveit, M.E., Jr. (1992). Ethylene in Plant Biology, 2nd ed. (San Diego, CA: Academic Press).

Achard, P., Baghour, M., Chapple, A., Hedden, P., Van der Straeten, D., Genschik, P., Moritz, T., and Harberd, N.P. (2007). The plant stress hormone ethylene controls floral transition via DELLA-dependent regulation of floral meristem-identity genes. Proc. Natl. Acad. Sci. USA **104:** 6484–6489.

Aida, M., Ishida, T., and Tasaka, M. (1999). Shoot apical meristem and cotyledon formation during Arabidopsis embryogenesis, interaction among the CUP-SHAPED COYLEDON and SHOOT MERISTEMLESS genes. Development **126:** 1563–1570.

Aida, M., Ishida, T., Fukaki, H., Fujisawa, H., and Tasaka, M. (1997). Genes involved in organ separation in Arabidopsis: an analysis of cup-shaped cotyledon mutant. Plant Cell **9:** 841–857.

Alonso, J.M., Stepanova, A.N., Solano, R., Wisman, E., Ferrari, S., Ausubel, F.M., and Ecker, J.R. (2003). Five components of fthe ethylene-response pathway identified in a screen for weak ethylene-insensitive mutants in Arabidopsis. Proc. Natl. Acad. Sci. USA **100:** 2992–2997.

Araki, T., and Komeda, Y. (1993). Analysis of the role of the late-flowering locus GI in the flowering of *Arabidopsis thaliana*. Plant J. **3:** 231–239.

Beck, E., and Ziegler, P. (1989). Biosynthesis and degradation of starch in higher plants. Annu. Rev. Plant Physiol. Plant Mol. Biol. **40:** 95–117.

Binder, B.M., O'Malley, R.C., Wang, W., Moore, J.M., Parks, B.M., Spalding, E.P., and Bleecker, A.B. (2004). Arabidopsis seedling growth response and recovery to ethylene. A kinetic analysis. Plant Physiol. **136:** 2913–2920.

Bleecker, A.B., Estelle, M.A., Somerville, C., and Kende, H. (1988). Insensitivity to ethylene conferred by a dominant mutation in *Arabidopsis thaliana*. Science **241:** 1086–1089.

Bleecker, A.B., and Kende, H. (2000). Ethylene: A gaseous signal molecule in plants. Annu. Rev. Cell Dev. Biol. **16:** 1–18.

Cao, W.H. (2004). Ethylene Receptor Regulates Plant Response to Salt Stress. PhD dissertation (Beijing, China: Institute of Genetics and Developmental Biology, Chinese Academy of Sciences).

Cao, W.H., Dong, Y., Zhang, J.S., and Chen, S.Y. (2003). Characterization of an ethylene receptor homolog gene from rice. Sci. China **46:** 370–378.

Cao, W.H., Liu, J., He, X.J., Mu, R.L., Zhou, H.L., Chen, S.Y., and Zhang, J.S. (2007). Modulation of ethylene responses affects plant salt-stress responses. Plant Physiol. **143:** 707–719.

Cao, W.H., Liu, J., Zhou, Q.Y., Cao, Y.R., Zheng, S.F., Du, B.X., Zhang, J.S., and Chen, S.Y. (2006). Expression of tobacco ethylene receptor NTHK1 alters plant responses to salt stress. Plant Cell Environ. **29:** 1210–1219.

Chang, C., Kwok, S.F., Bleecker, A.B., and Meyerowitz, E.M. (1993). Arabidopsis ethylene response gene *ETR1*: Similarity of product to two-component regulators. Science **262:** 539–544.

Chen, S.Y., Zhu, L.H., Hong, J., and Chen, S.L. (1991). Molecular biological identification of rice salt tolerant line. Acta Bot. Sin. **33:** 569–573.

Chen, T. (2008). Signal Transduction and Domain Functional Analysis of Plant Ethylene Receptors. PhD dissertation (Beijing, China: Institute of Genetics and Developmental Biology, Chinese Academy of Sciences).

Chen, T., and Zhang, J.S. (2006). Ethylene biosynthesis and signal pathway model. Chinese Bull. Bot. **23:** 519–530.

Chen, Y.F., Etheridge, N., and Schaller, E. (2005). Ethylene signal transduction. Ann. Bot. (Lond.) **95:** 901–915.

Chen, Y.F., Randlett, M.D., Findell, J.L., and Schaller, G.E. (2002). Localization of the ethylene receptor ETR1 to the endoplasmic reticulum of Arabidopsis. J. Biol. Chem. **277:** 19861–19866.

Chen, Y.F., Shakeel, S.N., Bowers, J., Zhao, X.C., Etheridge, N., and Schaller, G.E. (2007). Ligand-induced degradation of the ethylene receptor ETR2 through a proteasome-dependent pathway in Arabidopsis. J. Biol. Chem. **282:** 24752–24758.

Cho, Y.H., and Yoo, S.D. (2007). ETHYLENE RESPONSE 1 histidine kinase activity of Arabidopsis promotes plant growth. Plant Physiol. **143:** 612–616.

Ciardi, J.A., Tieman, D.M., Lund, S.T., Jones, J.B., Stall, R.E., and Klee, H.J. (2000). Response to *Xanthomonas campestris* pv. *vesicatoria* in tomato involves regulation of ethylene receptor gene expression. Plant Physiol. **123:** 81–92.

Cicirelli, M.F., Pelech, S.L., and Krebs, E.G. (1988). Activation of multiple protein kinase during the burst in protein phosphorylation that precedes the first meiotic cell division in Xenopus oocytes. J. Biol. Chem. **263:** 2009–2019.

De Paepe, A., and Van Der Straeten, D. (2005). Ethylene biosynthesis and signaling: An overview. Vitam. Horm. **72:** 399–430.

Dong, C.H., Rivarola, M., Resnick, J.S., Maggin, B.D., and Chang, C. (2008). Subcellular co-localization of Arabidopsis RTE1 and ETR1 supports a regulatory role for RTE1 in ETR1 ethylene signaling. Plant J. **53:** 275–286.

Eimert, K., Wang, S.M., Lue, W., and Chen, J. (1995). Monogenic recessive mutations causing both late floral initiation and excess starch accumulation in Arabidopsis. Plant Cell **7:** 1703–1712.

Fukao, T., Xu, K., Ronald, P., and Bailey-Serres, J. (2006). A variable cluster of ethylene response factor–like genes regulates metabolic and developmental acclimation responses to submergence in rice. Plant Cell **18:** 2021–2034.

Gagne, J.M., Smalle, J., Gingerich, D.J., Walker, J.M., Yoo, S.D., Yanagisawa, S., and Vierstra, R.D. (2004). Arabidopsis EIN3-binding F-box1 and 2 from ubiquitin-protein ligases that repress ethylene action and promote growth by directing EIN3 degradation. Proc. Natl. Acad. Sci. USA **101:** 6803–6808.

Gallie, D.R., and Young, T.E. (2004). The ethylene biosynthetic and perception machinery is differentially expressed during endosperm and embryo development in maize. Mol. Genet. Genomics **271:** 267–281.

Gamble, R.L., Coonfield, M.L., and Schaller, G.E. (1998). Histidine kinase activity of the ETR1 ethylene receptor from Arabidopsis. Proc. Natl. Acad. Sci. USA **95:** 7825–7829.

Gao, Z., Wen, C.K., Binder, B.M., Chen, Y.F., Chang, J., Chiang, Y.H., Kerris III, R.J., Chang, C., and Schaller, G.E. (2008). Heteromeric interactions among ethylene receptors mediate signaling in Arabidopsis. J. Biol. Chem. **283:** 23801–23810.

Guo, H., and Ecker, J.R. (2003). Plant responses to ethylene gas are mediated by SCF(EBF1/EBF2)-dependent proteolysis of EIN3 transcription factor. Cell **115:** 667–677.

Guo, H., and Ecker, J.R. (2004). The ethylene signaling pathway: New insights. Curr. Opin. Plant Biol. **7:** 40–49.

Hall, B.P., Shakeel, S.N., and Schaller, G.E. (2007). Ethylene receptors: Ethylene perception and signal transduction. J. Plant Growth Regul. **26:** 118–130.

Hass, C., Lohrmann, J., Albrecht, V., Sweere, U., Hummel, F., Yoo, S.D., Hwang, I., Zhu, T., Schafer, E., Kudla, J., and Harter, K. (2004). The response regulator 2 mediates ethylene signaling and hormone signal integration in Arabidopsis. EMBO J. **18:** 3290–3302.

Hayama, R., Yokoi, S., Tamaki, S., Yano, M., and Shimamoto, K. (2003). Adaptation of photoperiodic control pathways produces short-day flowering in rice. Nature **422:** 719–722.

He, X.J., Mu, R.L., Cao, W.H., Zhang, Z.G., Zhang, J.S., and Chen, S.Y. (2005). AtNAC2, a transcription factor downstream of ethylene and auxin signaling pathways, is involved in salt stress response and lateral root development. Plant J. **44:** 903–916.

He, X.J., Zhang, Z.G., Yan, D.Q., Zhang, J.S., and Chen, S.Y. (2004). A salt-responsive receptor-like kinase gene regulated by the ethylene signaling pathway encodes a plasma membrane serine/threonine kinase. Theor. Appl. Genet. **109:** 377–383.

Hirayama, T., Kieber, J.J., Hirayama, N., Kogan, M., Guzman, P., Nourizadeh, S., Alonso, J.M., Dailey, W.P., Dancis, A., and Ecker, J.R. (1999). RESPONSIVE-TO-ANTAGONIST1, a Menkes/Wilson disease-related copper transporter, is required for ethylene signaling in Arabidopsis. Cell **97:** 383–393.

Hua, J., and Meyerowitz, E.M. (1998). Ethylene responses are negatively regulated by a receptor gene family in *Arabidopsis thaliana*. Cell **94:** 261–271.

Hua, J., Sakai, H., Nourizadeh, S., Chen, Q.G., Bleecker, A.B., Ecker, J.R., and Meyerowitz, E.M. (1998). *EIN4* and *ERS2* are members of the putative ethylene receptor gene family in Arabidopsis. Plant Cell **10:** 1321–1332.

Jun, S.H., Han, M.J., Lee, S., Seo, Y.S., Kim, W.T., and An, G. (2004). OsEIN2 is a positive component in ethylene signaling in rice. Plant Cell Physiol. **45:** 281–289.

Kevany, B.M., Tieman, D.M., Taylor, M.G., Cin, V.D., and Klee, H.J. (2007). Ethylene receptor degradation controls the timing of ripening in tomato fruit. Plant J. **51:** 458–467.

Klee, H.J. (2002). Control of ethylene-mediated processes in tomato at the level of receptors. J. Exp. Bot. **53:** 2057–2063.

Klee, H.J. (2004). Ethylene signal transduction. Moving beyond Arabidopsis. Plant Physiol. **135:** 660–667.

Knoester, M., van Loon, L.C., van den Henvel, J., Henning, J., Bol, J.F., and Linthhorst, H.J.M. (1998). Ethylene-insensitive tobacco lacks nonhost resistance against soil-born fungi. Proc. Natl. Acad. Sci. USA **95:** 1933–1937.

Kobayashi, Y., Kaya, H., Goto, K., Iwabuchi, M., and Aradi, T. (1999). A pair of related genes with antagonistic roles in mediating flowering signals. Science **286:** 1960–1962.

Ku, H.S., Suge, H., Rappaport, L., and Pratt, H.K. (1970). Stimulation of rice coleoptile growth by ethylene. Planta **90:** 333–339.

Lanahan, M.B., Yen, H.C., Giovannoni, J.J., and Klee, H.J. (1994). The never ripe mutation blocks ethylene perception in tomato. Plant Cell **6:** 521–530.

Larsen, P.B., and Cancel, J.D. (2003). Enhanced ethylene responsiveness in the Arabidopsis eer1 mutant results from a loss-of-function mutation in the protein phosphatase 2A A regulatory subunit, RCN1. Plant J. **34:** 709–718.

Ma, B., Cui, M.L., Sun, H.J., Takada, K., Mori, H., Kamada, H., and Ezura, H. (2006). Subcellular localization and membrane topology of the melon ethylene receptor CmERS1. Plant Physiol. **141:** 587–597.

Ma, Q.H., and Wang, X.M. (2003). Characterization of an ethylene receptor homologue from wheat and its expression during leaf senescence. J. Exp. Bot. **54:** 1489–1490.

Maclean, J.L., Dawe, D.C., Hardy, B., and Hettel, G.P. (2002). Rice Almanac, 3rd ed. Los Banos (Philipines): International Rice Research Institute. Bouake (Cote d'Ivoire): West Africa Rice Development Association. Cali (Colombia): International Center for Tropical Agriculture. Rome (Italy): Food and Agriculture Organization. (Wallingford, UK: CABI Publishing).

Mao, C., Wang, S., Jia, Q., and Wu, P. (2006). *OsEIL1*, a rice homolog of the Arabidopsis EIN3 regulates the ethylene response as a positive component. Plant Mol. Biol. **61:** 141–152.

Morgan, P.W., and Drew, M.C. (1997). Ethylene and plant responses to stress. Physiol. Plant. **100:** 620–630.

Moshkov, I.E., Mur, L.A.J., Novikova, G.V., Smith, A.R., and Hall, M.A. (2003). Ethylene regulates monomeric GTP-binding protein gene expression and activity in Arabidopsis. Plant Physiol. **131:** 1–13.

Moussatche, P., and Klee, H.J. (2004). Autophosphorylation activity of the Arabidopsis ethylene receptor multigene family. J. Biol. Chem. **279:** 48734–48741.

Nakagawa, M., Shimamoto, K., and Kyozuka, J. (2002). Overexpression of *RCN1* and *RCN2*, rice *TERMINAL FLOWER 1/CENTRORADIALIS* homologs, confers delay of phase transition and altered panicle morphology in rice. Plant J. **29:** 743–750.

O'Donnell, P.J., Schmelz, E., Block, A., Miersch, O., Wasternack, C., Jones, J.B., and Klee, H.J. (2003). Mutiple hormones act sequentially to mediate a susceptible tomato pathogen defense response. Plant Physiol. **133:** 1181–1189.

Ogawara, T., Higashi, K., Kamada, H., and Ezura, H. (2003). Ethylene advances the transition from vegetative growth to flowering in *Arabidopsis thaliana*. J. Plant Physiol. **160:** 1335–1340.

Olmedo, G., Guo, H., Gregory, B.D., Nourizadeh, S.D., Aguilar-Henonin, L., Li, H., An, F., Guzman, P., and Ecker, J.R. (2006). ETHYLENE-INSENSITIVE5 encoes a 5′→3′ exoribonuclease required for regulation of the EIN3-targeting F-box proteins EBF1/2. Proc. Natl. Acad. Sci. USA **103:** 13286–13293.

O'Malley, R.C., Rodriguez, F.I., Esch, J.J., Binder, B.M., O'Donnell, P., Klee, H.J., and Bleecker, A.B. (2005). Ethylene-binding activity, gene expression levels, and receptor system output for ethylene receptor family members from Arabidopsis and tomato. Plant J. **41:** 651–659.

Pareek, A., Singh, A., Kumar, M., Kushwaha, H.R., Lynn, A.M., and Singla-Pareek, S.L. (2006). Whole-genome analysis of *Oryza sativa* reveals similar architecture of two-component signaling machinery with Arabidopsis. Plant Physiol. **142:** 380–397.

Parkinson, J.S., and Kofoid, E.C. (1992). Communication modules in bacterial signaling proteins. Annu. Rev. Genet. **26:** 71–112.

Pierik, R., Tholen, D., Poorter, H., Visser, E.J.W., and Voesenek, L.A.C.J. (2006). The Janus face of ethylene: growth inhibition and stimulation. Trends Plant Sci. **11:** 176–183.

Potuschak, T., Lechner, E., Parmentier, Y., Yanagisawa, S., Grava, S., Koncz, C., and Genschik, P. (2003). EIN3-dependent regulation of plant ethylene hormone signaling by two Arabidopsis F box proteins: EBF1 and EBF2. Cell **115:** 679–689.

Potuschak, T., Vansiri, A., Binder, B.M., Lechner, E., Vierstra, R.D., and Genschik, P. (2006). The exoribonuclease XRN4 is a component of the ethylene response pathway in Arabidopsis. Plant Cell **18:** 3047–3057.

Qiao, H., Chang, K.N., Yazaki, J., and Ecker, J.R. (2009). Interplay between ethylene, ETP1/ETP2 F-box proteins, and degradation of EIN2 triggers ethylene responses in Arabidopsis. Genes Dev. **23:** 512–521.

Qu, X., and Schaller, G.E. (2004). Requirement of the histidine kinase

domain for signal transduction by the ethylene receptor ETR1. Plant Physiol. **136:** 2961–2970.

Quaked, F., Rozhon, W., Lecourieux, D., and Hirt, H. (2003). A MAPK pathway mediates ethylene signaling in plants. EMBO J. **22:** 1282–1288.

Resnick, J.S., Rivarola, M., and Chang, C. (2008). Involvement of RTE1 in conformational changes promoting ETR1 ethylene receptor signaling in Arabidopsis. Plant J. **56:** 423–431.

Resnick, J.S., Wen, C.K., Shockey, J.A., and Chang, C. (2006). *REVERSION-TO-ETHYLENE SENSITIVITY1*, a conserved gene that regulates ethylene receptor function in Arabidopsis. Proc. Natl. Acad. Sci. USA **103:** 7917–7922.

Rieu, I., Wolters-Arts, M., Derksen, J., Mariani, C., and Weterings, K. (2003). Ethylene regulates the timing of anther dehiscence in tobacco. Planta **217:** 131–137.

Rijpkema, A.S., Gerats, T., and Vandenbussche, M. (2007). Evolutionary complexity of MADS complexes. Curr. Opin. Plant Biol. **10:** 32–38.

Rodriguez, F.I., Esch, J.J., Hall, A.E., Binder, B.M., Schaller, G.E., and Bleecker, A.B. (1999). A copper cofactor for the ethylene receptor ETR1 from Arabidopsis. Science **283:** 996–998.

Robinson, V.L., Buckler, D.R., and Stock, A.M. (2000). A tale of two-components: A novel kinase and a regulatory switch. Nat. Struct. Biol. **7:** 626–633.

Sato-Nara, K., Yuhashi, K., Higashi, K., Hosoya, K., Kubota, M., and Ezura, H. (1999). Stage- and tissue-specific expression of ethylene receptor homolog genes during fruit development in Muskmelon. Plant Physiol. **119:** 321–329.

Schaller, G.E., and Bleecker, A.B. (1995). Ethylene-binding sites generated in yeast expressing the Arabidopsis ETR1 gene. Science **270:** 1809–1811.

Tieman, D.M., Taylor, M.G., Ciardi, J.A., and Klee, H.J. (2000). The tomato ethylene receptors NR and LeETR4 are negative regulators of ethylene response and exhibit functional compensation within a multigene family. Proc. Natl. Acad. Sci. USA **97:** 5663–5668.

Trusov, Y., and Botella, J.R. (2006). Silencing of the ACC synthase gene ACACS2 causes delayed floweing in pineapple *Ananas comosus* (L.) Merr. J. Exp. Bot. **57:** 3953–3960.

van Loon, L.C., Geraats, B.P., and Linthorst, H.J. (2006). Ethylene as a modulator of disease resistance in plants. Trends Plant Sci. **11:** 184–191.

Wang, K.L.C., Li, H., and Ecker, J.R. (2002). Ethylene biosynthesis and signaling networks. Plant Cell **14**(suppl.): S131–S151.

Wang, W., Esch, J.J., Shiu, S.H., Agula, H., Binder, B.M., Chang, C., Patterson, S.E., and Bleecker, A.B. (2006). Identification of important regions for ethylene binding and signaling in the transmembrane domain of the ETR1 ethylene receptor of *Arabidopsis*. Plant Cell **18:** 3429–3442.

Wang, W., Hall, A.E., O'Malley, R., and Bleecker, A.B. (2003). Canonical histidine kinase activity of the transmitter domain of the ETR1 ethylene receptor from Arabidopsis is not required for signal transmission. Proc. Natl. Acad. Sci. USA **100:** 352–357.

Watanabe, H., Saigusa, M., Hase, S., Hayakawa, T., and Satoh, S. (2004). Cloning of a cDNA encoding an ETR2-like protein (Os-ERL1) from deep water rice (Oryza sativa L.) and increase in its mRNA level by submergence, ethylene, and gibberellin treatments. J. Exp. Bot. **55:** 1145–1148.

Wurgler-Murphy, S.M., and Saito, H. (1997). Two-component signal transducers and MAPK cascades. Trends Biochem. Sci. **22:** 172–176.

Xie, C., Zhang, J.S., Zhou, H.L., Li, J., Zhang, Z.G., Wang, D.W., and Chen, S.Y. (2003). Serine/threonine kinase activity in the putative histidine kinase-like ethylene receptor NTHK1 from tobacco. Plant J. **33:** 385–393.

Xie, C., Zhang, Z.G., Zhang, J.S., He, X.J., Cao, W.H., He, S.J., and Chen, S.Y. (2002). Spatial expression and characterization of a putative ethylene receptor protein NTHK1 in tobacco. Plant Cell Physiol. **43:** 810–815.

Xie, F., Liu, Q., and Wen, C.K. (2006). Receptor signal output mediated by the ETR1 N terminus is primarily subfamily I receptor dependent. Plant Physiol. **142:** 492–508.

Yamasaki, S., Fujii, N., and Takahashi, H. (2000). The ethylene-regulated expression of CS-ETR2 and CS-ERS genes in cucumber plants and their possible involvement with sex expression in flowers. Plant Cell Physiol. **41:** 608–616.

Yang, J., Zhang, J., Wang, Z., Liu, K., and Wang, P. (2006). Post-anthesis development of inferior and superior spikelets in rice in relation to abscisic acid and ethylene. J. Exp. Bot. **57:** 149–160.

Yau, C.P., Wang, L., Yu, M., Zee, S.Y., and Yip, W.K. (2004). Differential expression of three genes encoding an ethylene receptor in rice during development, and in response to indole-3-acetic acid and silver ions. J. Exp. Bot. **55:** 547–556.

Yoo, S.D., Cho, Y.H., Tena, G., Xiong, Y., and Sheen, J. (2008). Dual control of nuclear EIN3 by bifurcate MAPK cascades in C2H4 signaling. Nature **451:** 789–795.

Zhang, J.S., Xie, C., Du, B.X., Wu, X.L., and Chen, S.Y. (2001b). Tobacco two-component gene NTHK2. Chin. Sci. Bull. **46:** 574–577.

Zhang, J.S., Xie, C., Li, Z.Y., and Chen, S.Y. (1999b). Expression of the plasma membrane H^+-ATPase gene in response to salt stress in a rice salt-tolerant mutant and its original variety. Theor. Appl. Genet. **99:** 1006–1011.

Zhang, J.S., Xie, C., Liu, F., Liu, F.H., and Chen, S.Y. (1999a). A novel tobacco gene coding for a product similar to bacterial two-component regulators. Chin. Sci. Bull. **44:** 1025–1029.

Zhang, J.S., Xie, C., Shen, Y.G., and Chen, S.Y. (2001a). A two-component gene (NTHK1) encoding a putative ethylene-receptor homolog is both developmentally and stress-regulated in tobacco. Theor. Appl. Genet. **102:** 815–824.

Zhang, J.S., Zhou, J.M., Zhang, C., and Chen, S.Y. (1996). Differential gene expression in salt-tolerant rice mutant and its parental variety. Sci. China **39:** 310–319.

Zhang, Z.G., Zhou, H.L., Chen, T., Gong, Y., Cao, W.H., Wang, Y.J., Zhang, J.S., and Chen, S.Y. (2004). Evidence for serine/threonine and hsitidine kinase activity in the tobacco ethylene receptor protein NTHK2. Plant Physiol. **136:** 2971–2981.

Zheng, Q., and Wang, X.J. (2008). GOEAST: A web-based software toolkit for gene ontology enrichment analysis. Nucleic Acids Res. **36:** W358–W363.

Zhou, H.L., Cao, W.H., Cao, Y.R., Liu, J., Hao, Y.J., Zhang, J.S., and Chen, S.Y. (2006a). Roles of ethylene receptor NTHK1 domains in plant growth, stress response and protein phosphorylation. FEBS Lett. **580:** 1239–1250.

Zhou, H.L., He, S.J., Cao, Y.R., Chen, T., Du, B.X., Chu, C.C., Zhang, J.S., and Chen, S.Y. (2006b). OsGLU1, a putative membrane-bound endo-1,4-β-D- glucanase from rice, affects plant internode elongation. Plant Mol. Biol. **60:** 137–151.

Zhou, X., Liu, Q., Xie, F., and Wen, C.K. (2007). RTE1 is a golgi-associated and ETR1-dependent negative regulator of ethylene responses. Plant Physiol. **145:** 75–86.